THE ASTROPHYSICAL JOURNAL, 435:647–667, 1994 November 10

THE PRIMORDIAL HELIUM ABUNDANCE FROM A NEW SAMPLE OF METAL-DEFICIENT BLUE COMPACT GALAXIES

YURI I. IZOTOV
Main Astronomical Observatory, Ukrainian Academy of Sciences, Goloseevo, Kiev 252127, Ukraine

TRINH X. THUAN[1]
Astronomy Department, University of Virginia, and DAEC, Observatoire de Paris-Meudon, Meudon 92195 CEDEX, France

AND

VALENTIN A. LIPOVETSKY[1]
Special Astrophysical Observatory, Russian Academy of Sciences, Nizhny Arkhyz, Karachai-Circessia 357147, Russia
Received 1993 December 2; accepted 1994 May 11

ABSTRACT

We use high-quality spectrophotometric observations of 10 low-metallicity blue compact galaxies (BCGs) with oxygen abundance ranging from 12 + log(O/H) = 7.37 to 8.04 to determine the primordial helium abundance. We take special care into investigating the physical effects which may affect such a determination. We find that underlying stellar absorption, enhancement of helium lines due to self-absorption, and corrections for neutral and doubly ionized helium to be negligible. The main physical mechanism changing the He I line intensities from their recombination values is collisional excitation. To correct for it, we calculate the electron number density in the He^+ zone by a self-consistent procedure which constrains the He I λ5876/λ4471, λ6678/λ4471 and λ7065/λ4471 line ratios to have their recombination values, after correction for collisional enhancement. The density sensitive He I λ7065 line plays an important role in this respect. The usual practice of using the electron number density derived from the [S II] λ6717/λ6731 ratio underestimates the collisional enhancement correction and hence overestimates the helium abundance by $\sim$5%. We find that Brocklehurst's (1972) He I recombination emissivities give a smaller dispersion of the data points in the Y versus O/H and Y versus N/H planes and within the derived He abundances from different lines in a given galaxy than Smits's old (1991a, b) emissivities. The dispersion is comparable when Smits's new (1994) emissivities are used.

By taking the mean of the intercepts of both Y versus O/H and Y versus N/H linear regressions at O/H = N/H = 0, we determine a primordial helium mass fraction $Y_p = 0.229 \pm 0.004$, with Brocklehurst's emissivities, and $Y_p = 0.240 \pm 0.005$ with Smits's new emissivities. Taking the mean Y of the four most metal-deficient BCGs ($Z < Z_\odot/15$) in our sample gives $Y_p = 0.233 \pm 0.003$ with Brocklehurst's emissivities. Adding the four known BCGs with $Z < Z_\odot/15$ from the literature yields: $Y_p = 0.232 \pm 0.002$. These determinations are consistent with the lower limit of $Y_p = 0.236$ required by standard big bang nucleosynthesis theory. We obtain a slope $dY/dZ = 5.8 \pm 1.7$ with Brocklehurst's emissivities and $dY/dZ = 5.8 \pm 4.4$ with Smits' new emissivities, larger than the values predicted by closed-box models, but consistent with those given by chemical evolution models with differential galactic winds.

Subject headings: galaxies: abundances — galaxies: compact — galaxies: evolution — galaxies: ISM — H II regions

1. INTRODUCTION

Helium is the second most abundant element in the universe. Produced mainly in the first few hundred seconds of the universe, its abundance has increased at most by 10%–20% during subsequent stellar nucleosynthesis, making possible a precise determination of its primordial value. Such a determination is of special interest because standard big bang nucleosynthesis (SBBN) theory predicts the primordial abundance relative to hydrogen of ^{4}He (and of the other light elements D, ^{3}He, and ^{7}Li) to be a function of a single cosmological parameter, the baryon-to-photon ratio. The ratio, equal to a few $\times 10^{-10}$, is related, through the temperature of the microwave background radiation, to the mean baryonic mass density of the universe. Thus, estimates of lower and upper limits to the primordial abundances of the light elements, and of ^{4}He in particular, establish corresponding limits to the baryonic mass density of the universe. Moreover, Y_p depends sensitively on two physical constants, the lifetime of the neutron τ_n and the number of neutrino families n_ν (Olive et al. 1990; Walker et al. 1991; Pagel et al. 1992). Recent particle physics experiments indicate that $\tau_n = 889 \pm 3.5$ s (Walker et al. 1991) and $n_\nu = 3.01 \pm 0.10$ (Pagel et al. 1992). These values put a lower limit to the primordial helium mass fraction of $Y_p = 0.236 \pm 0.001$ (where the uncertainty reflects the experimental uncertainties in τ_n) for SBBN to be valid.

Therefore, an accurate determination of Y_p provides not only an important consistency test of SBBN theory, but also strong cosmological constraints on the values of the two physical constants n_ν and τ_n (Pagel et al. 1992, and references therein).

There exists a vast literature on helium abundance determination in different astrophysical objects. However, the majority of these determinations are subject to systematic errors and most objects contain nonprimordial helium produced by stellar nucleosynthesis. Since a precision of a few percent in Y_p

[1] Visiting Astronomer, Kitt Peak National Optical Observatories, operated by the Association of Universities for Research in Astronomy, Inc., under contract with the National Science Foundation.

is necessary to distinguish between different nucleosynthesis cosmological models (Pagel et al. 1992), the most appropriate objects in which to carry out the determination of Y_p are blue compact galaxies (BCGs). These dwarf systems ($M_B \geq -18$) are the least chemically evolved galaxies known ($Z_\odot/50 \leq Z \leq Z_\odot/3$) so that they contain very little helium manufactured by stars after the big bang. Moreover, they are undergoing an intense burst of star formation (see Thuan 1991 for a review) giving rise to high excitation supergiant H II regions, which allows an accurate determination of the helium abundance in the ionized gas, through the BCG emission-line spectra. The theory of nebular emission is simple and well-understood enough to yield, in principle, the required accuracy.

Peimbert & Torres-Peimbert (1974, 1976) first noted the correlation between helium and oxygen abundances in a small sample of dwarf magellanic irregulars and BCGs and they proposed to determine Y_p by linear extrapolation of the correlation to O/H = 0. Later, Pagel, Terlevich & Melnick (1986) proposed to use also the Y versus N/H correlation to determine Y_p, to take into account the temporary local excess of helium and nitrogen due to pollution by winds from massive stars. Many attempts at determining Y_p have been made, using the Y versus O/H and Y versus N/H correlations on various samples of dwarf irregulars and BCGs (Lequeux et al. 1979; French 1980; Kinman & Davidson 1981; Kunth & Sargent 1983; Davidson & Kinman 1985; Campbell, Terlevich, & Melnick 1986; Peimbert, Peña, & Torres-Peimbert 1986; Dufour, Garnett & Shields 1988; Vilchez et al. 1988; Torres-Peimbert, Peimbert, & Fierro 1989; Olive et al. 1990; Pagel & Simonson 1991; Terlevich et al. 1991; Melnick, Heydary-Malayeri & Leisy 1992; Pagel et al. 1992; Skillman & Kennicutt 1993).

The most accurate and consistent data set to-date is that by Pagel et al. (1992). They obtained $Y_p = 0.228 \pm 0.005$, using both the Y versus O/H and Y versus N/H regression lines. This value is uncomfortably close to the lower limit of $Y_p = 0.236$ allowed by SBBN theory. Thus it is critical to obtain another measurement of Y_p with as high or better precision from an independent data set to test SBBN theory.

To achieve such an aim, we need a reasonably large sample ($\sim$10 or more) of BCGs with low metallicity ($Z \leq Z_\odot/10$). For a long time, the known number of such metal-deficient BCGs was very small. For more than 20 years, I Zw 18 stood by itself at $Z \sim Z_\odot/50$ (Searle & Sargent 1972), with a large gap in the BCG metallicity distribution between $Z_\odot/15$ and $Z_\odot/50$. However, during the last few years, new BCGs have been discovered in the First and Second Byurakan objective prism Surveys with metallicities approaching or close to that of I Zw 18 (Izotov et al. 1990a, b, 1991). Subsequent observations of some of these galaxies (Terlevich et al. 1991; Melnick et al. 1992) have confirmed their extremely low metallicities. These low-metallicity BCGs appear to be ideal for a new determination of Y_p.

Besides the adequacy of the sample, there are questions about the validity of the very procedure for determining Y_p. The latter is customarily determined by linear extrapolation of the Y versus O/H and Y versus N/H relations toward zero O/H and N/H. Only closed-box chemical evolution models for BCGs with the instantaneous recycling approximation predict such a linear relation. Yet, there are both observational evidence and theoretical arguments which suggest that BCGs are not closed-box systems, but that they lose mass via galactic winds. On the observational side, there is the discovery in some dwarf irregular and blue compact galaxies of fast gas motion ($\sim$1000–2000 km s^{-1}) far in excess of the typical dwarf galaxy escape velocity of $\sim$100 km s^{-1} (Roy et al. 1992; Izotov et al. 1992b; Thuan et al. 1994). On the theoretical side, chemical evolution models by Pilyugin (1993) and Marconi, Matteucci, & Tosi (1994), which include the selective loss of heavy elements via a galactic wind, predict Y versus O/H and Y versus N/H tracks which are unique for each galaxy, depending on its mass loss efficiency and thus cast doubt on an universal linear relationship for Y versus O/H and Y versus N/H. Recognizing the effect of galactic winds which would lead to an upward dispersion in Y for a given O/H, Campbell (1992) has suggested fitting instead to the lower envelope of the Y versus O/H relation to determine Y_p.

Finally, there is the problem of the accuracy of the atomic data for the He atom. Differences in the values of the He recombination emissivities by Brocklehurst (1972), Smits (1991a, b) and Smits (1994) can lead to differences in Y_p of at least 4%–5% (Skillman & Kennicutt 1993).

We present in this paper high signal-to-noise ratio spectrophotometric observations of a sample of 10 low-metallicity ($Z_\odot/35 \leq Z \leq Z_\odot/7$) BCGs. The observations are used for a determination of the primordial helium abundance. In § 2, we describe the observations and data reduction. In § 3, we determine the physical conditions and heavy element abundances in the BCG star-forming regions. In § 4, helium abundance determinations are discussed. We pay particular attention to the different physical mechanisms and atomic data which may affect the He recombination line intensities. We determine the primordial helium abundance in § 5, using two different methods. We summarize our conclusions in § 6.

2. OBSERVATIONS AND DATA REDUCTION

High signal-to-noise ratio spectrophotometric observations of 10 BCGs were obtained with the Kitt Peak 4 meter Mayall telescope on the nights of 1993 March 23–24. Nine BCGs were selected from a complete sample of $\sim$450 BCGs (Izotov et al. 1992a) discovered in the First and Second Byurakan objective prism surveys (Markarian 1967; Markarian, Lipovetsky, & Stepanian 1983; Markarian et al. 1989). They were chosen to have a metallicity lower than $\sim Z_\odot/10$. Metallicities were estimated from low signal-to-noise Russian 6 m telescope spectra. An additional galaxy, UGC 4483 ≡ 0832 + 699, was also included because its brightest H II region has a very low metal content ($Z \sim Z_\odot/20$) (Izotov et al. 1992c). The general properties of the observed galaxies are given in Table 1.

All observations were made with the Ritchey-Chretien RC2 spectrograph used in conjunction with the T2KB 2048 × 2048 CCD detector. We use a 2″ × 300″ slit with the KPC-10A grating (316 lines mm^{-1}) in first order, with a GG 385 order separation filter. This filter cuts off all second-order flux contamination for wavelengths blueward of 7200 Å, which is the wavelength region of interest here. The above instrumental set-up gave a spatial scale along the slit of 0.69 arcsec pixel^{-1}, a scale perpendicular to the slit of 3.7 Å pixel^{-1}, a spectral range of 3500–7500 Å and a spectral resolution of $\sim$7 Å. These parameters permitted to cover simultaneously the blue and red spectral range with all the lines of interest and with enough spectral resolution to separate such important lines as [O III] λ4363 and [N II] λ6584. The seeing was typically 1″.5–2″. Both nights were transparent, so that absolute spectrophotometry

TABLE 1

GENERAL PARAMETERS OF GALAXIES

Name	Coordinates (1950.0) α	δ	m_{pg}	Angular diameter[a]	z	M^b_{pg}	Other names[c]	Ref.[d]
0832+699	$08^h32^m00.0^s$	+69°54′00″	14.9	10[e]	0.0009	−12.9	UGC 4483	1
0940+544N	09 40 50.4	+54 25 28	17.3	4	0.0055	−14.7		2
0946+558	09 46 03.1	+55 48 46	15.8	13×17	0.0053	−15.8	Mrk 22	2,3
0948+532	09 48 16.7	+53 13 00	18.0	6	0.0463	−18.5		2
1135+581	11 35 51.3	+58 09 24	15.5	13	0.0034	−15.2	Mrk 1450	2,4
1152+579	11 52 52.1	+57 56 26	16.5	7	0.0172	−17.7	Mrk 193	5
1159+545	11 59 29.0	+54 32 33	18.0	5	0.0119	−15.5		2
1211+540	12 11 33.9	+54 01 58	17.8	8	0.0031	−12.9		2
1331+493	13 31 20.4	+49 21 35	15.0	24×18	0.0020	−15.2		2
1437+370	14 37 03.0	+37 01 07	17.0	10	0.0014	−12.9	Mrk 475	6

[a] In arcsecs.
[b] All objects are assumed to be at their redshift distances with $H_0 = 75$ km s^{-1} Mpc^{-1}, except for 0832+699 in the M81 group for which a distance of 3.5 Mpc was adopted.
[c] Blank entries are SBS objects.
[d] (1) Izotov et al. 1992c; (2) Izotov et al. 1991, 1992a; (3) Markarian 1967; (4) Markarian et al. 1981; (5) Markarian 1969; (6) Markarian & Lipovetsky 1972.
[e] Diameter of the brightest H II region.

was possible. Exposure times were long enough, so that He I λ6678 line, the weakest line used in the helium abundance determination, had at least a signal-to-noise ratio of 10. Total exposure times typically ranged between 30 and 60 minutes. Generally, each exposure was broken up into 2 or 3 subexposures not exceeding 20 minutes, to allow for cosmic ray removal. All objects were observed at airmasses less than 1.3, so that no correction was made for atmospheric dispersion. The log of the observations is given in Table 2. Three Kitt Peak IRS spectrophotometric standard stars were observed each night for flux calibration. Spectra of He-Ne-Ar comparison arcs were obtained before and after each observation to calibrate the wavelength scale.

Preliminary data reduction was carried out at the NOAO headquarters in Tucson using the IRAF software package. This included bias subtraction, cosmic-ray removal and flat-fielding by using exposures obtained with a quartz lamp. After correcting for atmospheric extinction, wavelength and flux calibrating, the night sky background was subtracted from each frame. Final reduction was carried out at the Special Astrophysical Observatory using the MIDAS software package. We extracted one-dimensional spectra by summing 5 pixel rows along the slit, corresponding to an angular size of 3″.5, about the size of the brightest part of the H II regions in our BCGs. The spectra of all 10 galaxies are shown in Figures 1 and 2. The line identifications are given in the spectrum of 1152+579 in Figure 1. We note that, because of the very high signal-to-noise ratio, many weak lines seldom seen before in published BCG spectra are detected. For example, the [Cl III] λ5518, 5538 and [Fe III] λ4658 lines are present. A polynomial was fitted iteratively to the continuum after removal of the emission lines, and line intensities were measured by fitting Gaussian profiles.

TABLE 2

JOURNAL OF OBSERVATIONS

Galaxy	Date	No. of exp.	Total exp. (min)	Airmass
0832+699	March 23,1993	3	30	1.33
0940+544N	March 24	3	60	1.14
0946+558	March 23	2	30	1.22
0948+532	March 24	1	15	1.08
1135+581	March 24	3	30	1.15
1152+579	March 24	3	45	1.11
1159+545	March 24	3	60	1.11
1211+540	March 23	3	60	1.11
1331+493	March 23	3	45	1.18
1437+370	March 24	2	35	1.08

The observed line intensities given in Table 3 were corrected for both reddening and underlying stellar absorption. Some authors (McCall, Rybski, & Shields 1985; Skillman & Kennicutt 1993) have adopted a constant equivalent width (2 Å) for the hydrogen absorption lines. Because the real value of the absorption equivalent width is uncertain and dependent on the age of the star formation burst, we have adopted an iterative procedure to derive simultaneously both the extinction coefficient $C(\mathrm{H}\beta)$ and the absorption equivalent width for the hydrogen lines from the equation

$$\frac{I(\lambda)}{I(\mathrm{H}\beta)} = \frac{\mathrm{EW}_e(\lambda) + \mathrm{EW}_a(\lambda)}{\mathrm{EW}_e(\lambda)} \frac{\mathrm{EW}_e(\mathrm{H}\beta)}{\mathrm{EW}_e(\mathrm{H}\beta) + \mathrm{EW}_a(\mathrm{H}\beta)} \times \frac{F(\lambda)}{F(\mathrm{H}\beta)} \exp\left[C(\mathrm{H}\beta) f(\lambda)\right] , \quad (1)$$

where $I(\lambda)$ is the intrinsic line flux and $F(\lambda)$ is the observed line flux corrected for atmospheric extinction. $\mathrm{EW}_e(\lambda)$ and $\mathrm{EW}_a(\lambda)$ are, respectively, the equivalent widths of the observed emission line and of the underlying absorption line, $f(\lambda)$ is the reddening function, normalized at Hβ, which we take from Whitford (1958), and which can be approximated in the whole spectral range with an accuracy better than 5% by

$$f(\lambda) = 3.15854 \times 10^{-1.02109\lambda} - 1 \quad (2)$$

in which λ is in units of μm.

For the intrinsic hydrogen line intensity ratios, we used the theoretical ratios from Brocklehurst (1971) at the electron temperature estimated from the observed [O III] (λ4959 + λ5007)/λ4363 ratio. For lines other than that of hydrogen, $\mathrm{EW}_a(\lambda) = 0$

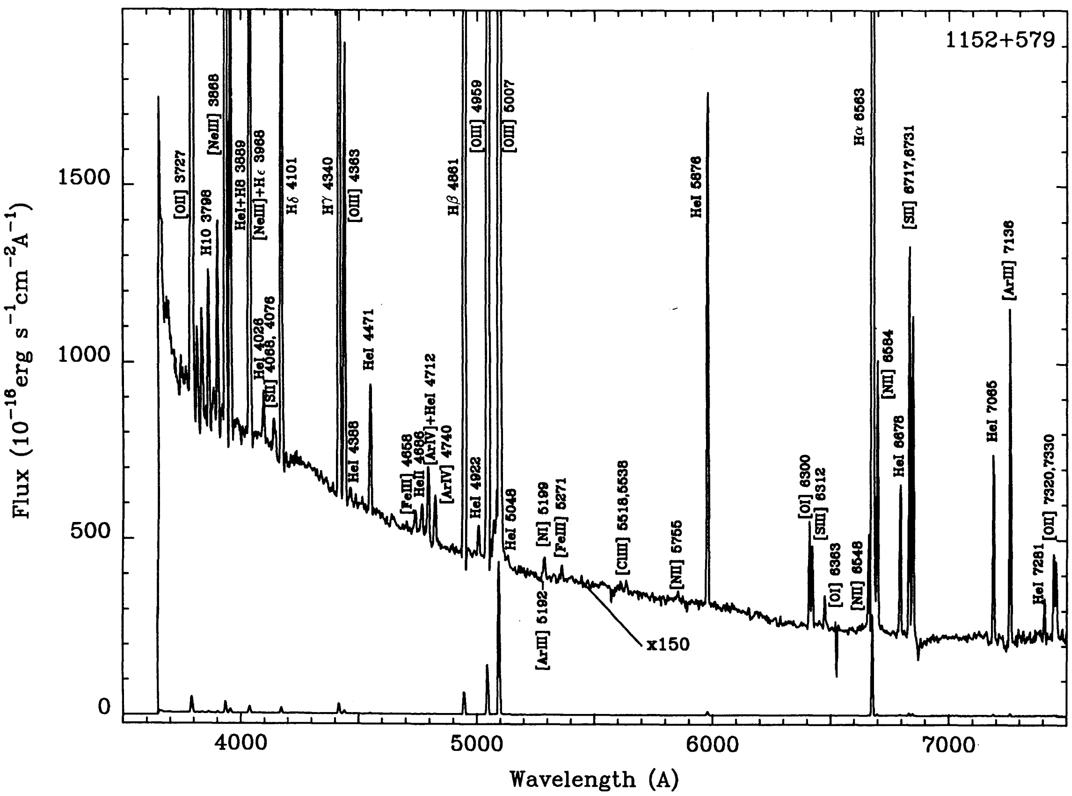

FIG. 1.—Mayall 4 m spectrum of one the 10 blue compact galaxies in our sample: 1152+579 ≡ Mrk 193. Identifications for the emission lines are given. Note the broad ($\Delta v \sim 2000$ km s^{-1}) low intensities components of the [O III] λ5007 and Hα λ6563 emission lines, indicative of galactic winds.

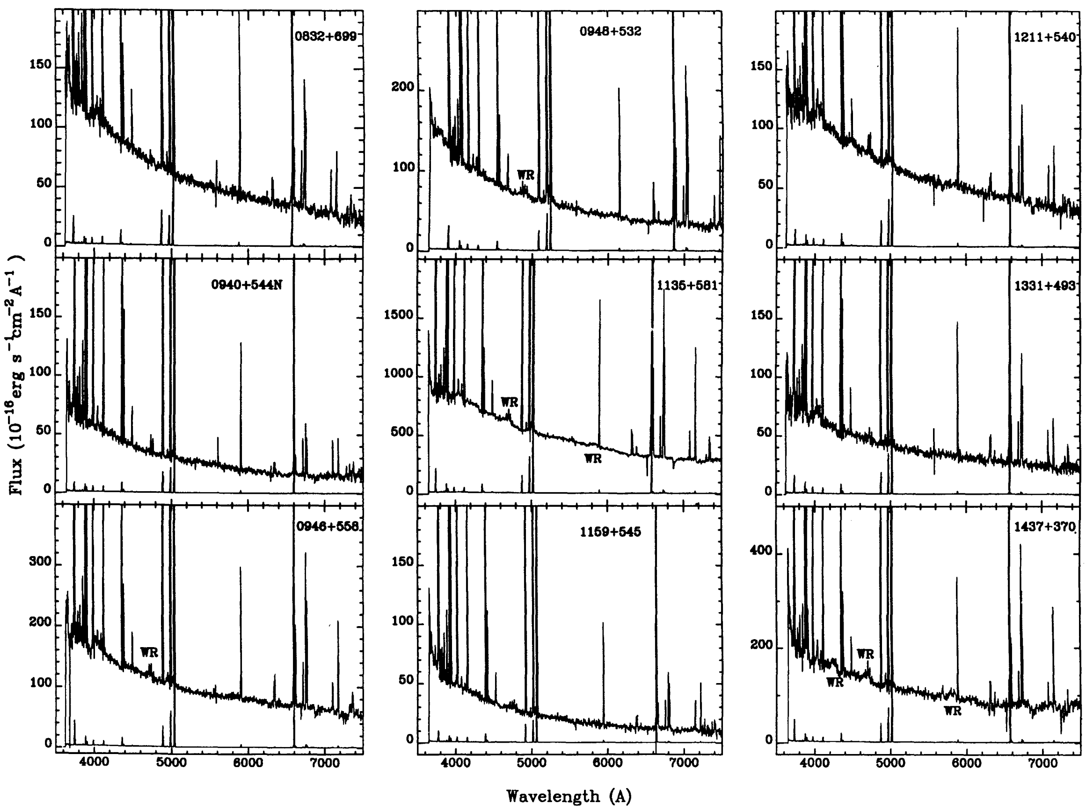

FIG. 2.—Spectra of the other nine galaxies in our blue compact galaxy sample. Note the Wolf-Rayet features in 0946+558, 0948+532, 1135+581, and 1437+370. Note also the low-intensity broad component in the Hα λ6563 line in 0940+544N and 1135+581.

TABLE 3

EMISSION LINE INTENSITIES

Ion	0832+699 F(λ)/F(Hβ)	0832+699 I(λ)/I(Hβ)	0940+544N F(λ)/F(Hβ)	0940+544N I(λ)/I(Hβ)
	Galaxy			
3727 [O II]	0.922±0.017	1.055±0.019	0.505±0.018	0.505±0.018
3750 H12	0.020±0.004	0.037±0.009	0.015±0.004	0.015±0.004
3771 H11	0.030±0.004	0.048±0.007	0.028±0.005	0.028±0.005
3798 H10	0.035±0.004	0.053±0.006	0.043±0.005	0.043±0.005
3820 He I	...	...	0.012±0.003	0.012±0.003
3835 H9	0.053±0.004	0.073±0.006	0.072±0.006	0.072±0.006
3868 [Ne III]	0.214±0.005	0.240±0.006	0.373±0.012	0.373±0.012
3889 H8 + He I	0.161±0.005	0.193±0.006	0.205±0.009	0.205±0.009
3968 H7 + [Ne III]	0.188±0.005	0.220±0.006	0.286±0.009	0.286±0.009
4026 He I	0.011±0.002	0.012±0.002	0.021±0.003	0.021±0.003
4068 [S II]	0.013±0.002	0.014±0.002	0.005±0.002	0.005±0.002
4101 Hδ	0.234±0.005	0.266±0.006	0.270±0.008	0.270±0.009
4340 Hγ	0.429±0.006	0.463±0.007	0.519±0.012	0.519±0.012
4363 [O III]	0.064±0.002	0.067±0.002	0.136±0.005	0.136±0.005
4388 He I	...	...	...	...
4471 He I	0.036±0.002	0.038±0.002	0.038±0.003	0.038±0.003
4658 [Fe III]	...	...	0.004±0.001	0.004±0.001
4686 He II	...	...	...	...
4713 [Ar IV] + He I	0.008±0.001	0.008±0.001	0.015±0.002	0.015±0.002
4740 [Ar IV]	...	...	0.011±0.002	0.011±0.002
4861 Hβ	1.000±0.010	1.000±0.010	1.000±0.017	1.000±0.017
4922 He I	0.010±0.001	0.010±0.001	0.006±0.001	0.006±0.001
4959 [O III]	0.955±0.009	0.939±0.009	1.372±0.022	1.372±0.022
5007 [O III]	2.881±0.023	2.818±0.022	3.390±0.047	3.390±0.047
5199 [N I]	...	...	...	...
5518 [Cl III]	...	...	...	...
5538 [Cl III]	...	...	...	...
5755 [N II]	...	...	...	...
5876 He I	0.109±0.003	0.099±0.002	0.106±0.004	0.106±0.004
6300 [O I]	0.016±0.001	0.014±0.001	0.010±0.002	0.010±0.002
6312 [S III]	0.014±0.001	0.012±0.001	0.011±0.001	0.011±0.001
6363 [O I]	...	...	...	...
6563 Hα	3.260±0.025	2.783±0.024	2.682±0.038	2.682±0.038
6584 [N II]	0.034±0.002	0.029±0.001	0.016±0.002	0.016±0.002
6678 He I	0.032±0.002	0.027±0.001	0.027±0.002	0.027±0.002
6717 [S II]	0.075±0.002	0.064±0.002	0.042±0.003	0.042±0.003
6731 [S II]	0.057±0.002	0.048±0.002	0.033±0.003	0.033±0.003
7065 He I	0.025±0.002	0.020±0.001	0.029±0.003	0.029±0.003
7136 [Ar III]	0.044±0.002	0.036±0.002	0.031±0.003	0.031±0.003
7281 He I	...	...	0.007±0.002	0.007±0.002
7320 [O II]	0.010±0.002	0.008±0.001	0.008±0.002	0.008±0.002
7330 [O II]	0.011±0.002	0.009±0.001	0.011±0.002	0.011±0.002
C(Hβ) mag	0.200		0.000	
F(Hβ)(×10^{14}) erg s^{-1} cm^{-2} $Å^{-1}$	2.2		1.5	
EW(Hβ) Å	169		235	
EW(abs) Å	1.1		0.0	

Ion	0946+558 F(λ)/F(Hβ)	0946+558 I(λ)/I(Hβ)	0948+532 F(λ)/F(Hβ)	0948+532 I(λ)/I(Hβ)
	Galaxy			
3727 [O II]	1.321±0.020	1.487±0.023	1.335±0.022	1.367±0.024
3750 H12	0.022±0.004	0.042±0.009	0.010±0.003	0.018±0.006
3771 H11	0.026±0.004	0.047±0.008	0.019±0.003	0.027±0.005
3798 H10	0.040±0.004	0.062±0.007	0.043±0.004	0.052±0.005
3820 He I	0.021±0.003	0.023±0.003	0.016±0.002	0.017±0.003
3835 H9	0.063±0.004	0.087±0.006	0.062±0.004	0.071±0.005
3868 [Ne III]	0.429±0.008	0.474±0.010	0.471±0.011	0.480±0.011
3889 H8 + He I	0.173±0.005	0.207±0.007	0.211±0.007	0.223±0.007
3968 H7 + [Ne III]	0.259±0.006	0.300±0.007	0.302±0.008	0.315±0.008
4026 He I	0.012±0.002	0.013±0.002	0.012±0.002	0.012±0.002
4068 [S II]	0.011±0.002	0.011±0.002	0.015±0.002	0.015±0.002
4101 Hδ	0.229±0.005	0.262±0.006	0.267±0.007	0.277±0.007
4340 Hγ	0.429±0.006	0.462±0.007	0.470±0.009	0.479±0.010
4363 [O III]	0.078±0.003	0.082±0.003	0.082±0.003	0.083±0.004
4388 He I	0.003±0.001	0.003±0.001	...	...
4471 He I	0.039±0.002	0.040±0.002	0.041±0.003	0.041±0.003
4658 [Fe III]	...	...	0.007±0.001	0.007±0.001
4686 He II	0.016±0.001	0.017±0.001	0.010±0.001	0.010±0.001
4713 [Ar IV] + He I	0.019±0.001	0.019±0.001	0.011±0.001	0.011±0.001
4740 [Ar IV]	0.008±0.001	0.008±0.001	...	...
4861 Hβ	1.000±0.010	1.000±0.011	1.000±0.015	1.000±0.015
4922 He I	0.011±0.001	0.010±0.001	0.011±0.002	0.011±0.002
4959 [O III]	1.859±0.016	1.824±0.016	1.821±0.024	1.810±0.024
5007 [O III]	5.585±0.043	5.455±0.042	5.673±0.065	5.632±0.064
5199 [N I]	0.004±0.001	0.003±0.001	0.004±0.001	0.004±0.001
5518 [Cl III]	0.005±0.001	0.005±0.001	0.008±0.001	0.008±0.001
5538 [Cl III]	...	...	...	...
5755 [N II]	...	...	...	...
5876 He I	0.121±0.003	0.110±0.003	0.113±0.004	0.111±0.004
6300 [O I]	0.022±0.002	0.019±0.001	0.031±0.002	0.030±0.002
6312 [S III]	0.027±0.002	0.024±0.001	0.020±0.002	0.019±0.002
6363 [O I]	0.007±0.001	0.006±0.001	0.011±0.002	0.010±0.002
6563 Hα	3.266±0.027	2.825±0.025	2.915±0.036	2.818±0.034
6584 [N II]	0.074±0.002	0.064±0.002	0.070±0.003	0.068±0.003
6678 He I	0.034±0.002	0.029±0.002	0.030±0.002	0.029±0.002
6717 [S II]	0.134±0.003	0.114±0.003	0.144±0.005	0.138±0.005
6731 [S II]	0.100±0.003	0.085±0.002	0.107±0.004	0.103±0.004
7065 He I	0.029±0.002	0.024±0.002	0.027±0.003	0.026±0.003
7136 [Ar III]	0.078±0.003	0.065±0.002	0.083±0.005	0.080±0.005
7281 He I	0.006±0.002	0.005±0.002	...	...
7320 [O II]	0.020±0.002	0.016±0.002	...	...
7330 [O II]	0.024±0.002	0.020±0.002	...	...
C(Hβ) mag	0.180		0.040	
F(Hβ)(×10^{14}) erg s^{-1} cm^{-2} $Å^{-1}$	2.6		2.1	
EW(Hβ) Å	125		164	
EW(abs) Å	1.2		0.7	

TABLE 3—*Continued*

Ion	1135+581 F(λ)/F(Hβ)	1135+581 I(λ)/I(Hβ)	1152+579 F(λ)/F(Hβ)	1152+579 I(λ)/I(Hβ)
3727 [O II]	1.244±0.012	1.346±0.013	0.745±0.011	0.887±0.014
3750 H12	0.007±0.002	0.042±0.016	0.015±0.002	0.041±0.006
3771 H11	0.019±0.002	0.043±0.008	0.021±0.002	0.048±0.006
3798 H10	0.025±0.002	0.061±0.006	0.034±0.002	0.062±0.005
3820 He I	0.025±0.002	0.027±0.002	0.014±0.002	0.017±0.002
3835 H9	0.045±0.002	0.082±0.004	0.046±0.002	0.075±0.004
3868 [Ne III]	0.441±0.005	0.471±0.006	0.476±0.007	0.552±0.009
3889 H8 + He I	0.150±0.003	0.191±0.004	0.161±0.004	0.206±0.005
3968 H7 + [Ne III]	0.249±0.003	0.296±0.005	0.291±0.005	0.351±0.007
4026 He I	0.018±0.001	0.018±0.001	0.016±0.001	0.018±0.002
4068 [S II]	0.011±0.001	0.012±0.001	0.011±0.001	0.013±0.001
4101 Hδ	0.235±0.003	0.277±0.004	0.243±0.004	0.288±0.005
4340 Hγ	0.432±0.004	0.469±0.005	0.434±0.006	0.481±0.007
4363 [O III]	0.068±0.002	0.069±0.002	0.132±0.003	0.140±0.003
4388 He I	0.002±0.001	0.002±0.001	0.003±0.001	0.003±0.001
4471 He I	0.037±0.001	0.037±0.001	0.037±0.002	0.039±0.002
4658 [Fe III]	0.011±0.001	0.011±0.001	0.007±0.001	0.007±0.001
4686 He II	0.019±0.001	0.019±0.001	0.012±0.001	0.012±0.001
4713 [Ar IV] + He I	0.014±0.001	0.014±0.001	0.021±0.001	0.021±0.001
4740 [Ar IV]	0.007±0.001	0.007±0.001	0.012±0.001	0.012±0.001
4861 Hβ	1.000±0.006	1.000±0.006	1.000±0.010	1.000±0.010
4922 He I	0.009±0.001	0.008±0.001	0.011±0.001	0.011±0.001
4959 [O III]	1.841±0.010	1.791±0.010	2.161±0.018	2.112±0.018
5007 [O III]	4.916±0.024	4.765±0.024	6.224±0.046	6.043±0.045
5199 [N I]	0.003±0.001	0.003±0.001	0.006±0.001	0.005±0.001
5518 [Cl III]	0.004±0.001	0.004±0.001	0.002±0.001	0.002±0.001
5538 [Cl III]	0.002±0.001	0.002±0.001	0.002±0.001	0.002±0.001
5755 [N II]	0.001±0.001	0.001±0.001	0.002±0.001	0.002±0.001
5876 He I	0.122±0.002	0.112±0.002	0.128±0.003	0.111±0.002
6300 [O I]	0.023±0.001	0.021±0.001	0.024±0.001	0.020±0.001
6312 [S III]	0.017±0.001	0.015±0.001	0.019±0.001	0.016±0.001
6363 [O I]	0.008±0.001	0.008±0.001	0.007±0.001	0.006±0.001
6563 Hα	3.041±0.016	2.827±0.016	3.431±0.027	2.791±0.024
6584 [N II]	0.076±0.002	0.067±0.001	0.049±0.002	0.040±0.002
6678 He I	0.032±0.001	0.028±0.001	0.035±0.002	0.028±0.001
6717 [S II]	0.134±0.002	0.117±0.002	0.085±0.002	0.068±0.002
6731 [S II]	0.095±0.002	0.083±0.002	0.068±0.002	0.054±0.002
7065 He I	0.025±0.001	0.022±0.001	0.041±0.002	0.032±0.002
7136 [Ar III]	0.098±0.002	0.084±0.002	0.070±0.003	0.054±0.002
7281 He I	0.006±0.001	0.005±0.001	0.008±0.001	0.006±0.001
7320 [O II]	0.023±0.002	0.019±0.001	0.019±0.002	0.014±0.001
7330 [O II]	0.020±0.001	0.017±0.001	0.018±0.002	0.014±0.001
C(Hβ) mag	0.140		0.260	
F(Hβ)(×10^{14}) erg s^{-1} cm^{-2} Å^{-1}	14.0		6.0	
EW(Hβ) Å	128		204	
EW(abs) Å	2.6		1.9	

Ion	1159+545 F(λ)/F(Hβ)	1159+545 I(λ)/I(Hβ)	1211+540 F(λ)/F(Hβ)	1211+540 I(λ)/I(Hβ)
3727 [O II]	0.677±0.021	0.677±0.021	0.617±0.012	0.646±0.013
3750 H12	0.016±0.004	0.016±0.004	0.012±0.004	0.055±0.019
3771 H11	0.023±0.004	0.023±0.004	0.020±0.003	0.063±0.012
3798 H10	0.050±0.005	0.050±0.005	0.035±0.003	0.078±0.008
3820 He I	0.011±0.003	0.011±0.003	0.011±0.003	0.011±0.003
3835 H9	0.067±0.006	0.067±0.006	0.044±0.003	0.087±0.007
3868 [Ne III]	0.333±0.011	0.333±0.011	0.372±0.007	0.385±0.007
3889 H8 + He I	0.217±0.009	0.217±0.009	0.151±0.004	0.197±0.006
3968 H7 + [Ne III]	0.291±0.010	0.291±0.010	0.239±0.005	0.287±0.006
4026 He I	0.015±0.002	0.015±0.002	0.011±0.002	0.012±0.002
4068 [S II]	0.006±0.002	0.006±0.002	0.005±0.002	0.006±0.002
4101 Hδ	0.286±0.009	0.286±0.009	0.237±0.004	0.278±0.006
4340 Hγ	0.503±0.012	0.503±0.012	0.436±0.006	0.470±0.007
4363 [O III]	0.109±0.005	0.109±0.005	0.116±0.003	0.116±0.003
4388 He I	...	...	0.003±0.001	0.003±0.001
4471 He I	0.036±0.003	0.036±0.003	0.036±0.002	0.035±0.002
4658 [Fe III]	0.005±0.001	0.005±0.001	...	...
4686 He II	0.008±0.001	0.008±0.001	0.026±0.001	0.026±0.001
4713 [Ar IV] + He I	0.012±0.002	0.012±0.002	0.020±0.001	0.019±0.001
4740 [Ar IV]	0.007±0.001	0.007±0.001	0.006±0.001	0.006±0.001
4861 Hβ	1.000±0.018	1.000±0.018	1.000±0.009	1.000±0.009
4922 He I	0.006±0.001	0.006±0.001	...	...
4959 [O III]	1.124±0.020	1.124±0.020	1.584±0.013	1.537±0.013
5007 [O III]	3.460±0.050	3.460±0.050	4.803±0.034	4.648±0.034
5199 [N I]	...	...	...	...
5518 [Cl III]	...	...	...	...
5538 [Cl III]	...	...	...	...
5755 [N II]	0.003±0.001	0.003±0.001	...	...
5876 He I	0.099±0.004	0.099±0.004	0.107±0.002	0.099±0.002
6300 [O I]	0.011±0.002	0.011±0.002	0.013±0.001	0.012±0.001
6312 [S III]	0.012±0.002	0.012±0.002	0.016±0.001	0.015±0.001
6363 [O I]	0.004±0.001	0.004±0.001	0.003±0.001	0.003±0.001
6563 Hα	2.570±0.039	2.570±0.039	3.115±0.023	2.773±0.023
6584 [N II]	0.022±0.002	0.022±0.002	0.022±0.002	0.020±0.001
6678 He I	0.024±0.002	0.024±0.002	0.030±0.002	0.027±0.002
6717 [S II]	0.054±0.004	0.054±0.004	0.060±0.002	0.053±0.002
6731 [S II]	0.042±0.003	0.042±0.003	0.047±0.002	0.042±0.002
7065 He I	0.025±0.003	0.025±0.003	0.027±0.002	0.024±0.002
7136 [Ar III]	0.041±0.004	0.041±0.004	0.041±0.002	0.036±0.002
7281 He I	0.007±0.002	0.007±0.002	0.005±0.002	0.004±0.002
7320 [O II]	0.012±0.003	0.012±0.003	0.007±0.002	0.007±0.002
7330 [O II]	0.008±0.003	0.008±0.003	0.007±0.002	0.007±0.002
C(Hβ) mag	0.000		0.100	
F(Hβ)(×10^{14}) erg s^{-1} cm^{-2} Å^{-1}	1.3		2.0	
EW(Hβ) Å	254		138	
EW(abs) Å	0.0		3.5	

TABLE 3—*Continued*

Ion	1331+493N F(λ)/F(Hβ)	1331+493N I(λ)/I(Hβ)	1437+370 F(λ)/F(Hβ)	1437+370 I(λ)/I(Hβ)
3727 [O II]	0.799±0.017	0.886±0.020	1.277±0.023	1.401±0.026
3750 H12	0.010±0.004	0.028±0.013	0.004±0.005	0.016±0.027
3771 H11	0.023±0.004	0.042±0.008	0.012±0.005	0.026±0.012
3798 H10	0.037±0.004	0.057±0.007	0.029±0.005	0.043±0.008
3820 He I	0.014±0.003	0.015±0.003	...	...
3835 H9	0.056±0.004	0.077±0.006	0.047±0.005	0.062±0.007
3868 [Ne III]	0.450±0.009	0.491±0.010	0.430±0.010	0.466±0.011
3889 H8 + He I	0.165±0.005	0.195±0.007	0.200±0.007	0.226±0.008
3968 H7 + [Ne III]	0.267±0.006	0.304±0.008	0.254±0.007	0.283±0.008
4026 He I	0.014±0.002	0.016±0.002	0.025±0.003	0.027±0.003
4068 [S II]	0.006±0.002	0.006±0.002	0.016±0.003	0.017±0.003
4101 Hδ	0.242±0.005	0.272±0.007	0.238±0.006	0.262±0.007
4340 Hγ	0.437±0.007	0.466±0.008	0.448±0.008	0.473±0.009
4363 [O III]	0.117±0.003	0.121±0.004	0.085±0.003	0.088±0.004
4388 He I	0.007±0.002	0.008±0.002	0.006±0.002	0.006±0.002
4471 He I	0.036±0.002	0.037±0.002	0.036±0.003	0.037±0.003
4658 [Fe III]	...	...	...	...
4686 He II	...	...	0.029±0.002	0.029±0.002
4713 [Ar IV] + He I	0.011±0.001	0.011±0.002	0.017±0.002	0.017±0.002
4740 [Ar IV]	0.006±0.001	0.006±0.001	0.008±0.001	0.008±0.002
4861 Hβ	1.000±0.011	1.000±0.012	1.000±0.012	1.000±0.012
4922 He I	0.016±0.002	0.015±0.002	0.029±0.002	0.028±0.002
4959 [O III]	1.820±0.018	1.788±0.018	1.786±0.019	1.761±0.019
5007 [O III]	5.579±0.049	5.458±0.048	5.362±0.050	5.268±0.050
5199 [N I]	...	...	...	...
5518 [Cl III]	0.005±0.001	0.005±0.001	...	...
5538 [Cl III]	...	...	0.005±0.002	0.004±0.002
5755 [N II]	...	...	...	...
5876 He I	0.115±0.003	0.105±0.003	0.113±0.003	0.104±0.003
6300 [O I]	0.023±0.002	0.020±0.002	0.029±0.002	0.026±0.002
6312 [S III]	0.018±0.002	0.016±0.001	0.020±0.002	0.018±0.002
6363 [O I]	0.007±0.001	0.006±0.001	0.014±0.002	0.012±0.002
6563 Hα	3.067±0.029	2.788±0.029	3.148±0.031	2.813±0.031
6584 [N II]	0.037±0.002	0.032±0.002	0.066±0.003	0.059±0.003
6678 He I	0.031±0.002	0.027±0.002	0.033±0.002	0.029±0.002
6717 [S II]	0.078±0.003	0.067±0.002	0.152±0.004	0.134±0.004
6731 [S II]	0.061±0.003	0.053±0.002	0.106±0.004	0.094±0.003
7065 He I	0.026±0.002	0.022±0.002	0.022±0.003	0.019±0.002
7136 [Ar III]	0.043±0.003	0.037±0.002	0.105±0.004	0.091±0.004
7281 He I	0.010±0.002	0.010±0.002	0.012±0.003	0.011±0.002
7320 [O II]	0.019±0.002	0.019±0.002	0.015±0.003	0.013±0.003
7330 [O II]	0.012±0.002	0.012±0.002	...	...
C(Hβ) mag	0.160		0.140	
F(Hβ)(×10^{14}) erg s^{-1}cm^{-2}Å^{-1}	1.7		3.2	
EW(Hβ) Å	192		133	
EW(abs) Å	1.8		0.9	

and equation (1) reduces to the commonly used equation

$$\frac{I(\lambda)}{I(\mathrm{H}\beta)} = \frac{F(\lambda)}{F(\mathrm{H}\beta)} \exp\left[C(\mathrm{H}\beta) f(\lambda)\right] . \qquad (3)$$

The corrected line intensities, extinction coefficient $C(\mathrm{H}\beta)$, and equivalent widths of the hydrogen absorption stellar lines are given in Table 3, along with the uncorrected Hβ flux and Hβ equivalent width. In general, $C(\mathrm{H}\beta)$ and EW_a are small for the galaxies under study.

Our procedure for correcting for absorption works well in most cases as an examination of Table 3 shows. The intensities of the hydrogen lines which originate from high levels and which suffer most from absorption because of their low equivalent widths, agree well with theoretical predictions (Brocklehurst 1971; Aller 1984) in most galaxies. The exceptions are galaxies 0940+544N and 1159+545, where the intensity of Hγ was larger and that of Hα smaller than the theoretical values. Our described algorithm failed to find values for both EW_a and $C(\mathrm{H}\beta)$. We set them to be zero, since positive values for both quantities would make the discrepancy worse.

3. PHYSICAL CONDITIONS AND CHEMICAL COMPOSITION

3.1. *Electron Temperatures and Number Densities*

It is well known that the electron temperature T_e is different in high- and low-ionization zones of H II regions, especially in H II regions with low metallicity (Stasinska 1990). Since forbidden line intensities depend exponentially on T_e, it is extremely important for abundance determination to take the variation of T_e in the different zones within the H II region into account. All the spectra shown in Figures 1 and 2 have high signal-to-noise ratios, allowing the measurement of weak lines whose intensity can be as small as ∼0.5% of the Hβ intensity. Thus for some galaxies, it is possible, in principle, to use the following intensity ratios in the (N_e, T_e) plane to obtain both the electron number density N_e and the electron temperature T_e: the λ6717/λ6731 and (λ4068 + λ4076)/(λ6717 + λ6731) ratios for N_e(S II) and T_e(S II), the λ4363/(λ4959 + λ5007) ratio for T_e(O III), the λ5755/λ6584 ratio for T_e(N II), and the λ3727/(λ7320 + λ7330) ratio for T_e(O II). The last three ratios make use of the number density determined in the S II zone. Additionally for some objects in our sample, it is also possible to measure N_e(Ar IV) from the λ4711/λ4740 ratio. Since [Ar IV] λ4711 is contaminated with the He I λ4713 line, we have subtracted the latter adopting a He I λ4713/λ4471 recombination ratio of 0.092–0.139 which corresponds to T_e varying between 10,000 and 20,000 K (Aller 1984). However, because of the observational uncertainties introduced by the weakness of some of the concerned emission lines, their contamination by other lines (as for [Ar IV] λ4711) and the larger sensitivity to the uncertainty in the extinction coefficient when using ratios of widely separated lines (such as the [O II] lines), we have chosen to use the traditional method of determining T_e(O III) from the [O III] λ4363/(λ4959 + λ5007) ratio and N_e(S II) from the [S II] λ6717/λ6731 ratio, which relies on lines with high intensities. To take into account the electron temperatures for different ions, we have used the results of the H II photoionization models of Stasinska (1990). We can fit the results of her models with the following expressions:

$$t_e(\text{O II}) = 0.243 + t_e(\text{O III})[1.031 - 0.184 t_e(\text{O III})] , \quad (4)$$

$$t_e(\text{Ne III}) = t_e(\text{O III}) , \quad (5)$$

$$t_e(\text{N II}) = t_e(\text{O II}) , \quad (6)$$

$$t_e(\text{Fe III}) = t_e(\text{O II}) , \quad (7)$$

$$t_e(\text{He II}) = t_e(\text{O III}) , \quad (8)$$

where $t_e = T_e/10^4$ K.

Garnett (1992) has studied the behavior of T_e for different ions and has concluded that equations (5) and (6) are valid. He also examined the dependence of T_e(S III) and T_e(Ar III) on T_e(O III) and has derived the following relations which we adopt

$$t_e(\text{Ar III}) = 0.83 t_e(\text{O III}) + 0.17 , \quad (9)$$

$$t_e(\text{S III}) = t_e(\text{Ar III}) . \quad (10)$$

3.2. *Heavy Element Abundances*

To derive the ionic abundances, it has been assumed that the lines originate in two regions: a high-ionization zone with temperature T_e(O III), where O III, Ne III, and Ar IV lines originate, and a low-ionization zone with temperature T_e(O II), where O II, N II, S II, and Fe III lines originate. As for the Ar III and S III lines, they originate both in high- and low-ionization regions (Garnett 1992). Therefore, for these ions, the temperatures calculated from equations (9)–(10) are intermediate between T_e(O III) and T_e(O II). Since the electron number densities derived from the [S II] λ6717/λ6731 ratio are low (we set them to be equal to 100 cm^{-3} in most cases), the three-level atom solutions of McCall (1984) apply. For ionic abundance determination, except for the case of Fe^{++}, we used the expressions from Pagel et al. (1992) with modifications for S III, where T_e(S III) was used instead of T_e(O III). For Fe^{++}, using emissivities by Garstang, Robb, & Rountree (1978) we have derived

$$\frac{N(\text{Fe}^{++})}{N(\text{H}^+)} = 2.3 \times 10^{-6} E^0_{4,2} \sqrt{t}\, 10^{1.34/t} \frac{I(\lambda 4658)}{I(\text{H}\beta)} , \quad (11)$$

where

$$E^0_{4,2} = 1.387 t^{-0.983}\, 10^{-0.0424/t} \quad (12)$$

and $t = t_e$(Fe III). Ionic abundances are shown in Table 4, along with the electron temperatures for the different ions and the adopted electron number densities N_e(S II).

To obtain the total abundances of elements, it is necessary to take into account unseen stages of ionization. Then the total abundance of element A is equal to

$$\frac{A}{\text{H}} = \text{ICF}(A) \frac{A^{+i}}{\text{H}^+} , \quad (13)$$

where ICF(A) is the ionization correction factor for element A.

For oxygen, we adopted the following expression for the total abundance

$$\frac{\text{O}}{\text{H}} = \frac{\text{O}^+ + \text{O}^{++}}{\text{H}^+} . \quad (14)$$

In three of our galaxies, the nebular He II λ4686 line was detected. Therefore part of the oxygen in those BCGs is in the O^{+++} stage. However, the weakness of the He II λ4686 line means that the ionic abundance of O^{+++} does not exceed 2%–3% of the total oxygen abundance (Skillman & Kennicutt 1993). Therefore we do not take the O^{+++} ionic abundance into consideration.

For nitrogen and neon, we have used the following common expressions for the correction factors:

$$\text{ICF(N)} = \frac{\text{O}}{\text{O}^+} , \quad (15)$$

$$\text{ICF(Ne)} = \frac{\text{O}}{\text{O}^{++}} . \quad (16)$$

Garnett (1990) has studied the nitrogen ionic composition of giant H II regions in low-abundance irregular galaxies. In these galaxies, nitrogen is mostly in the N^{++} form. However, in nebulae having low abundances and/or ionizing stars hotter than 40,000 K, the N^+/O^+ is an accurate estimator of N/O. For these H II regions, Garnett (1990) using photoionization model calculations has obtained numerical coefficients ranging from 0.8 to 1.0 in equation (15). In order to compare our results with other data, we have set the coefficient to be 1.0 in equation (15).

Using Stasinska's (1990) photoionization H II models, we have derived the following expression for the ionization correction factor of Fe:

$$\text{ICF(Fe)} = \frac{\text{Fe}}{\text{Fe}^{++}} = 1.25 \frac{\text{O}}{\text{O}^+} . \quad (17)$$

Correction factors for Ar and S are more complex since both Ar^{++} and S^{++} exist in O^{++} and O^+ zones. Therefore, we have used the results of model calculations of photoionized H II

TABLE 4

IONIC AND TOTAL HEAVY ELEMENT ABUNDANCES

	Galaxy				
Property	0832+699	0940+544N	0946+558	0948+532	1135+581
T_e(OIII) (K)	15,800	20,400	13,000	12,900	12,700
T_e(OII) (K)	14,100	15,800	12,700	12,700	12,500
T_e(SIII) (K)	14,800	18,600	12,500	12,400	12,200
N_e(SII) (cm^{-3})	100	140	100	100	100
O^+/H^+ ($\times 10^4$)	0.11±0.01	0.04±0.00	0.22±0.01	0.20±0.01	0.21±0.01
O^{++}/H^+ ($\times 10^4$)	0.27±0.01	0.20±0.01	0.87±0.03	0.89±0.04	0.83±0.02
O/H ($\times 10^4$)	0.38±0.01	0.24±0.01	1.09±0.03	1.10±0.05	1.04±0.02
12+log(O/H)	7.58±0.02	7.37±0.02	8.04±0.01	8.04±0.02	8.02±0.01
N^+/H^+ ($\times 10^6$)	0.24±0.01	0.10±0.01	0.66±0.03	0.70±0.04	0.71±0.02
ICF	3.43	6.18	4.93	5.37	4.98
N/H ($\times 10^6$)	0.82±0.06	0.65±0.07	3.27±0.21	3.76±0.31	3.55±0.16
12+log(N/H)	5.91±0.03	5.81±0.05	6.52±0.03	6.58±0.04	6.55±0.02
Ne^{++}/H^+ ($\times 10^5$)	0.50±0.03	0.42±0.03	1.80±0.08	1.84±0.10	1.93±0.06
ICF	1.41	1.19	1.25	1.23	1.25
Ne/H ($\times 10^5$)	0.71±0.05	0.50±0.04	2.26±0.12	2.23±0.16	2.41±0.09
12+log(Ne/H)	6.85±0.03	6.70±0.04	7.35±0.02	7.35±0.03	7.38±0.02
S^+/H^+ ($\times 10^6$)	0.12±0.01	0.07±0.01	0.27±0.01	0.33±0.02	0.28±0.01
S^{++}/H^+ ($\times 10^6$)	0.63±0.06	0.31±0.04	2.22±0.15	1.80±0.18	1.56±0.09
ICF	1.36	1.78	1.58	1.65	1.58
S/H ($\times 10^6$)	1.02±0.07	0.68±0.06	3.92±0.19	3.50±0.24	2.91±0.11
12+log(S/H)	6.01±0.03	5.83±0.04	6.59±0.02	6.54±0.03	6.46±0.02
Ar^{++}/H^+ ($\times 10^7$)	1.31±0.06	0.79±0.07	3.30±0.12	4.05±0.25	4.41±0.09
Ar^{+++}/H^+ ($\times 10^7$)	...	0.82±0.13	1.63±0.25	...	1.48±0.16
ICF	1.60	1.02	1.04	1.98	1.03
Ar/H ($\times 10^7$)	2.10±0.08	1.65±0.15	5.10±0.29	8.00±0.35	6.10±0.19
12+log(Ar/H)	5.32±0.02	5.22±0.04	5.71±0.02	5.90±0.02	5.79±0.01
Fe^{++}/H^+ ($\times 10^6$)	...	0.06±0.02	...	0.22±0.04	0.34±0.02
ICF	...	7.73	...	6.71	6.22
Fe/H ($\times 10^6$)	...	0.47±0.06	...	1.44±0.11	2.13±0.06
12+log(Fe/H)	...	5.67±0.05	...	6.16±0.03	6.33±0.01

	Galaxy				
Property	1152+579	1159+545	1211+540	1331+493N	1437+370
T_e(OIII) (K)	15,500	18,300	16,200	15,400	13,600
T_e(OII) (K)	14,000	15,100	14,200	13,900	13,000
T_e(SIII) (K)	14,500	16,900	15,200	14,500	13,000
N_e(SII) (cm^{-3})	160	105	140	140	100
O^+/H^+ ($\times 10^4$)	0.10±0.03	0.06±0.00	0.07±0.00	0.10±0.01	0.19±0.01
O^{++}/H^+ ($\times 10^4$)	0.61±0.02	0.24±0.01	0.42±0.01	0.56±0.02	0.74±0.04
O/H ($\times 10^4$)	0.70±0.02	0.29±0.02	0.48±0.01	0.66±0.02	0.93±0.04
12+log(O/H)	7.85±0.01	7.47±0.02	7.68±0.01	7.82±0.01	7.97±0.02
N^+/H^+ ($\times 10^6$)	0.34±0.01	0.16±0.01	0.16±0.01	0.27±0.01	0.58±0.03
ICF	7.32	5.10	7.38	6.69	4.88
N/H ($\times 10^6$)	2.46±0.13	0.83±0.09	1.21±0.07	1.81±0.14	2.84±0.23
12+log(N/H)	6.39±0.02	5.92±0.05	6.08±0.03	6.26±0.03	6.45±0.04
Ne^{++}/H^+ ($\times 10^5$)	1.21±0.04	0.48±0.03	0.75±0.03	1.11±0.05	1.53±0.08
ICF	1.16	1.24	1.16	1.18	1.26
Ne/H ($\times 10^5$)	1.40±0.06	0.59±0.05	0.87±0.04	1.31±0.07	1.93±0.13
12+log(Ne/H)	7.15±0.02	6.77±0.04	6.94±0.02	7.12±0.02	7.29±0.03
S^+/H^+ ($\times 10^6$)	0.14±0.00	0.09±0.01	0.10±0.00	0.14±0.01	0.29±0.02
S^{++}/H^+ ($\times 10^6$)	0.86±0.05	0.45±0.07	0.73±0.06	0.92±0.09	1.51±0.16
ICF	1.97	1.60	1.98	1.87	1.57
S/H ($\times 10^6$)	1.96±0.07	0.87±0.08	1.65±0.09	1.98±0.12	2.83±0.20
12+log(S/H)	6.29±0.02	5.94±0.04	6.22±0.02	6.30±0.03	6.45±0.03
Ar^{++}/H^+ ($\times 10^7$)	2.03±0.01	1.22±0.11	1.27±0.07	1.41±0.09	4.30±0.17
Ar^{+++}/H^+ ($\times 10^7$)	1.60±0.13	0.67±0.14	...	...	1.50±0.27
ICF	1.02	1.03	2.34	2.22	1.04
Ar/H ($\times 10^7$)	3.69±0.15	1.95±0.18	2.98±0.11	3.13±0.13	6.01±0.32
12+log(Ar/H)	5.57±0.02	5.29±0.04	5.47±0.02	5.50±0.02	5.78±0.02
Fe^{++}/H^+ ($\times 10^6$)	0.15±0.02	0.08±0.02	...	...	...
ICF	9.15	6.37	...	...	...
Fe/H ($\times 10^6$)	1.41±0.50	0.53±0.06	...	...	...
12+log(Fe/H)	6.15±0.02	5.73±0.05	...	...	...

regions by Stasinska (1990). We obtained the following analytic approximations for ICF(S) and ICF(Ar):

$$\mathrm{ICF(S)} = \frac{\mathrm{S}}{\mathrm{S}^+ + \mathrm{S}^{++}} = [\![0.013 + x\{5.10 + x[-12.78 + x(14.77 - 6.11x)]\}]\!]^{-1}\,, \quad (18)$$

$$\mathrm{ICF(Ar)} = \frac{\mathrm{Ar}}{\mathrm{Ar}^{++} + \mathrm{Ar}^{+++}} = \{0.99 + x[0.091 + x(-1.14 + 0.077x)]\}^{-1}\,, \quad (19)$$

$$\mathrm{ICF(Ar)} = \frac{\mathrm{Ar}}{\mathrm{Ar}^{++}} = [0.15 + x(2.39 - 2.64x)]^{-1}\,, \quad (20)$$

where $x = \mathrm{O}^+/\mathrm{O}$.

The total heavy element abundances are shown in Table 4, along with adopted correction factors. In those cases when the [Ar IV] λ4740 line was not detected, equation (20) was used instead of equation (19). We draw attention to the very low metal content of some galaxies in our sample. The oxygen abundance in the two galaxies 0940+544N and 1159+545 are, respectively, 1/35 and 1/29 that of the Sun, very close to that in the two most metal-deficient BCGs known, I Zw 18 ($Z_\odot/50$) (Searle & Sargent 1972) and SBS 0335−052 ($Z_\odot/41$) (Izotov et al. 1990a, b; Melnick et al. 1992). The very low metallicity of the ionized gas in 0940+544N and 1159+545 has been noted before by Izotov et al. (1991) on the basis of lower signal-to-noise spectra. These low-metallicity galaxies will play a crucial role in the primordial helium abundance determination to be discussed next. A detailed analysis of the heavy element abundances will be given in a separate paper.

4. HELIUM ABUNDANCE DETERMINATION

Since our aim is to determine the helium primordial abundance Y_p to better than a few percent, we need to consider all the different factors which may affect the helium abundance determination at that precision level and take them into account. We shall discuss in turn: (1) the effect of using different sets of He I radiative recombination probabilities; (2) the self-absorption and collisional enhancement of He I lines; (3) the underlying stellar absorption and (4) the fraction of neutral helium.

4.1. *Brocklehurst (1972) versus Smits (1991a, b, 1994) Emissivities*

He emission-line strengths were converted to singly ionized helium $y^+ \equiv \mathrm{He}^+/\mathrm{H}^+$ and doubly ionized helium $y^{++} \equiv \mathrm{He}^{++}/\mathrm{H}^+$ abundances using the theoretical recombination emissivities by Brocklehurst (1971, 1972), and approximated by the following analytical expressions (Kunth & Sargent 1983):

$$y^+ = 2.04t^{0.13}\,\frac{I(\lambda4471)}{I(\mathrm{H}\beta)}\,, \quad (21)$$

$$y^+ = 0.738t^{0.23}\,\frac{I(\lambda5876)}{I(\mathrm{H}\beta)}\,, \quad (22)$$

$$y^+ = 2.58t^{0.25}\,\frac{I(\lambda6678)}{I(\mathrm{H}\beta)}\,, \quad (23)$$

$$y^{++} = 0.084t^{0.14}\,\frac{I(\lambda4686)}{I(\mathrm{H}\beta)}\,. \quad (24)$$

Newer H I and He II emissivities have been calculated by Hummer & Storey (1987), and He I emissivities by Smits (1991a, b, 1994). While Hummer & Storey (1987) emissivities are in excellent agreement with those of Brocklehurst (1971, 1972) for the range of temperature and density considered here, there is a difference of about 5% between Brocklehurst's and the first set of Smits's (1991a, b) emissivities for the He I λ5876 and λ6678 lines at T_e = 20,000 K, both of which are used for the determination of the helium abundance. Smits (1994) has recently calculated a new set of He I line emissivities. While the new emissivities agree well with those by Brocklehurst (1972) for the He I λ4471, λ5876, and λ6678 lines, that for the He I λ7065 line is ∼35% higher than Brocklehurst's value in the temperature range from 10,000 to 20,000 K. Using the old He I emissivities of Smits (1991a, b), Skillman & Kennicutt (1993) have derived the following expressions for the y^+ abundance determination, which we adopt:

$$y^+ = 2.03t^{0.149}\,\frac{I(\lambda4471)}{I(\mathrm{H}\beta)}\,, \quad (25)$$

$$y^+ = 0.753t^{0.270}\,\frac{I(\lambda5876)}{I(\mathrm{H}\beta)}\,, \quad (26)$$

$$y^+ = 2.63t^{0.283}\,\frac{I(\lambda6678)}{I(\mathrm{H}\beta)}\,. \quad (27)$$

For the new Smits (1994) emissivities, we use equations (21–23) to determine y^+. Table 5 shows the results for y^+ using Brocklehurst (1972) and both Smits's old (1991a, b) and new (1994) emissivities. Smits's emissivities give systematically higher y^+, by up to 10 percent for the old set, and by up to ∼7% for the new set. We shall discuss the effects of these differences on the primordial helium abundance determination in § 5.

4.2. *Self-absorption and Collisional Enhancement of* He I *Lines*

In the range of high temperatures found in our BCGs (Table 4), there are two main physical mechanisms which may make the He line intensities deviate from pure recombination values. The first mechanism is self-absorption in the He I λ3889 line. The second mechanism, also leading to the enhancement of some helium lines, is collisional excitation from the metastable $2\,^3S$ and $2\,^1S$ levels of He I.

We first estimate the self-absorption effect. As shown by Robbins (1968), self-absorption should lead to a decrease of the He I λ3889 line intensity. However, if we subtract from the He I + H8 λ3889 blend the H8 line with a recombination intensity of about 0.1 of the Hβ intensity, then the He I λ3889/λ4471 ratio has nearly recombination value for all galaxies.

We conclude that the effect of self-absorption on He I line intensities is negligible. This is in agreement with measurements of the He I λ7065 line which is most sensitive to self-absorption effects. Dinerstein & Shields (1986), Peimbert et al. (1986), Torres-Peimbert et al. (1989) and Pagel et al. (1992) have shown that, after correction for collisional excitation, the He I λ7065/λ4471 ratio is reduced from about 1 to 0.5, compared to a theoretical pure recombination ratio of 0.33. They also conclude that the self-absorption contribution to the He I λ4471, λ5876, and λ6678 lines is completely negligible.

We turn next to the discussion of the correction for collisional excitation of He I. We define a correction factor γ in the form:

$$y^+ = \frac{y^+(\mathrm{uncorrected})}{1+\gamma}\,. \quad (28)$$

TABLE 5

HELIUM ABUNDANCE

Property	Galaxy 0832+699	0940+544N	0946+558	0948+532	1135+581
Brocklehurst (1972):					
N_e(HeII)	250	400	750	1000	520
$(1+\gamma)(4471)$	1.032	1.104	1.040	1.049	1.027
$(1+\gamma)(5876)$	1.071	1.213	1.095	1.119	1.066
$(1+\gamma)(6678)$	1.025	1.066	1.037	1.046	1.026
$(1+\gamma)(7065)$	1.385	1.788	1.702	1.877	1.504
$y^+(4471)$	0.079±0.004	0.077±0.006	0.081±0.004	0.082±0.005	0.076±0.003
$y^+(5876)$	0.075±0.002	0.076±0.003	0.079±0.002	0.077±0.003	0.082±0.001
$y^+(6678)$	0.076±0.004	0.077±0.007	0.077±0.004	0.076±0.006	0.075±0.003
y^+(mean)	0.076±0.002	0.076±0.003	0.079±0.003	0.078±0.002	0.080±0.001
y^{++}	...	...	...	0.001±0.000	...
η^a	2.11	0.88	2.10	1.22	1.42
ICF	1.015	1.005	1.015	1.008	1.009
y	0.077±0.002	0.077±0.002	0.080±0.002	0.080±0.003	0.081±0.002
Y	0.236±0.007	0.235±0.009	0.242±0.007	0.241±0.009	0.243±0.006
Smits (1991a,b):					
N_e(HeII)	100	100	100	170	100
$(1+\gamma)(4471)$	1.014	1.029	1.007	1.011	1.006
$(1+\gamma)(5876)$	1.030	1.060	1.016	1.025	1.014
$(1+\gamma)(6678)$	1.011	1.019	1.006	1.010	1.006
$(1+\gamma)(7065)$	1.163	1.223	1.116	1.186	1.111
$y^+(4471)$	0.081±0.004	0.083±0.006	0.084±0.004	0.085±0.005	0.077±0.003
$y^+(5876)$	0.082±0.002	0.091±0.004	0.087±0.002	0.087±0.003	0.089±0.001
$y^+(6678)$	0.080±0.004	0.084±0.007	0.082±0.005	0.081±0.007	0.079±0.003
y^+(mean)	0.081±0.002	0.088±0.003	0.086±0.002	0.086±0.002	0.085±0.001
y	0.082±0.002	0.089±0.003	0.087±0.002	0.087±0.003	0.086±0.002
Y	0.248±0.007	0.262±0.010	0.258±0.007	0.259±0.009	0.255±0.006
Smits (1994):					
N_e(HeII)	100	100	160	270	100
$(1+\gamma)(4471)$	1.014	1.029	1.010	1.016	1.006
$(1+\gamma)(5876)$	1.030	1.060	1.025	1.039	1.014
$(1+\gamma)(6678)$	1.011	1.019	1.010	1.015	1.006
$(1+\gamma)(7065)$	1.163	1.223	1.182	1.289	1.111
$y^+(4471)$	0.080±0.004	0.082±0.006	0.084±0.004	0.085±0.005	0.078±0.003
$y^+(5876)$	0.078±0.002	0.087±0.003	0.084±0.002	0.084±0.003	0.086±0.001
$y^+(6678)$	0.077±0.004	0.080±0.007	0.079±0.004	0.078±0.006	0.077±0.003
y^+(mean)	0.078±0.002	0.085±0.003	0.083±0.002	0.083±0.002	0.083±0.001
y	0.078±0.002	0.085±0.003	0.083±0.002	0.085±0.003	0.084±0.002
Y	0.241±0.007	0.255±0.010	0.252±0.007	0.253±0.009	0.251±0.006
Brocklehurst (1972): (N_e(HeII)=N_e(SII))					
N_e(HeII)	100	140	100	100	100
$(1+\gamma)(4471)$	1.014	1.040	1.007	1.007	1.006
$(1+\gamma)(5876)$	1.030	1.081	1.016	1.016	1.014
$(1+\gamma)(6678)$	1.011	1.025	1.006	1.006	1.006
$y^+(4471)$	0.081±0.005	0.082±0.002	0.084±0.005	0.086±0.005	0.077±0.003
$y^+(5876)$	0.078±0.004	0.085±0.003	0.085±0.004	0.085±0.005	0.086±0.003
$y^+(6678)$	0.077±0.005	0.080±0.007	0.080±0.005	0.079±0.007	0.077±0.003
y^+(mean)	0.079±0.003	0.084±0.003	0.083±0.002	0.084±0.003	0.080±0.002
y	0.080±0.004	0.084±0.004	0.084±0.003	0.085±0.003	0.081±0.002
Y	0.242±0.011	0.252±0.010	0.252±0.009	0.254±0.012	0.244±0.007

TABLE 5—*Continued*

Property	Galaxy 1152+579	1159+545	1211+540	1331+493N	1437+370
Brocklehurst (1972):					
N_e(HeII)	1000	360	480	310	310
(1+γ)(4471)	1.096	1.070	1.062	1.035	1.022
(1+γ)(5876)	1.213	1.147	1.135	1.078	1.052
(1+γ)(6678)	1.075	1.049	1.047	1.028	1.020
(1+γ)(7065)	2.180	1.638	1.704	1.443	1.360
y^+(4471)	0.077±0.003	0.074±0.006	0.072±0.004	0.077±0.005	0.076±0.005
y^+(5876)	0.075±0.002	0.073±0.003	0.072±0.002	0.080±0.002	0.079±0.002
y^+(6678)	0.074±0.003	0.070±0.007	0.075±0.004	0.075±0.005	0.080±0.005
y^+(mean)	0.075±0.001	0.073±0.003	0.072±0.001	0.079±0.002	0.078±0.002
y^{++}	0.001±0.000	0.001±0.000	0.002±0.000	...	...
η^a	0.99	1.17	1.10	1.18	1.33
ICF	1.006	1.007	1.007	1.007	1.008
y	0.077±0.002	0.074±0.003	0.075±0.002	0.079±0.002	0.079±0.003
Y	0.235±0.006	0.229±0.010	0.231±0.007	0.240±0.008	0.240±0.008
Smits (1991a,b):					
N_e(HeII)	210	100	100	100	100
(1+γ)(4471)	1.026	1.022	1.015	1.012	1.008
(1+γ)(5876)	1.058	1.046	1.032	1.028	1.018
(1+γ)(6678)	1.020	1.015	1.011	1.010	1.007
(1+γ)(7065)	1.319	1.198	1.169	1.156	1.126
y^+(4471)	0.082±0.003	0.078±0.006	0.076±0.004	0.079±0.005	0.077±0.005
y^+(5876)	0.089±0.002	0.084±0.004	0.082±0.002	0.087±0.002	0.084±0.003
y^+(6678)	0.081±0.004	0.075±0.007	0.081±0.005	0.079±0.005	0.084±0.006
y^+(mean)	0.087±0.002	0.081±0.003	0.081±0.002	0.084±0.002	0.083±0.002
y	0.088±0.002	0.083±0.003	0.084±0.002	0.085±0.003	0.083±0.003
Y	0.261±0.007	0.248±0.010	0.251±0.007	0.253±0.008	0.250±0.008
Smits (1994):					
N_e(HeII)	290	100	100	100	100
(1+γ)(4471)	1.035	1.022	1.015	1.012	1.008
(1+γ)(5876)	1.078	1.046	1.032	1.028	1.018
(1+γ)(6678)	1.028	1.015	1.011	1.010	1.007
(1+γ)(7065)	1.430	1.198	1.169	1.156	1.126
y^+(4471)	0.082±0.003	0.077±0.006	0.076±0.004	0.079±0.005	0.077±0.005
y^+(5876)	0.085±0.002	0.080±0.004	0.079±0.002	0.083±0.002	0.081±0.002
y^+(6678)	0.078±0.004	0.072±0.007	0.078±0.005	0.077±0.005	0.081±0.006
y^+(mean)	0.083±0.002	0.078±0.003	0.079±0.002	0.082±0.002	0.081±0.002
y	0.085±0.002	0.079±0.003	0.081±0.002	0.082±0.003	0.081±0.003
Y	0.253±0.007	0.242±0.010	0.246±0.007	0.247±0.008	0.245±0.008
Brocklehurst (1972): (N_e(HeII)=N_e(SII))					
N_e(HeII)	160	105	140	140	100
(1+γ)(4471)	1.020	1.023	1.021	1.017	1.008
(1+γ)(5876)	1.045	1.048	1.045	1.037	1.018
(1+γ)(6678)	1.016	1.016	1.016	1.013	1.007
y^+(4471)	0.082±0.003	0.077±0.006	0.075±0.004	0.078±0.005	0.077±0.006
y^+(5876)	0.087±0.002	0.080±0.003	0.078±0.002	0.083±0.002	0.081±0.005
y^+(6678)	0.079±0.004	0.072±0.007	0.078±0.004	0.076±0.005	0.081±0.006
y^+(mean)	0.085±0.001	0.078±0.003	0.078±0.002	0.081±0.002	0.080±0.003
y	0.086±0.002	0.080±0.003	0.080±0.002	0.082±0.003	0.081±0.004
Y	0.257±0.007	0.242±0.010	0.243±0.007	0.246±0.008	0.243±0.011

[a] $\eta = (O^+/S^+)(S^{++}/O^{++})$ (Vilchez & Pagel 1988)

The enhancement factor $(1 + \gamma)$ of the helium lines is a function of electron temperature and number density in the He^+ region (Clegg 1987). From models of H II regions (Stasinska 1990), T_e(He II) ≈ T_e(O III). The electron number density N_e(He II) presents more of a problem. First, in the low-density (~100 cm^{-3}) regime, the [S II] λ6717/λ6731 ratio is a very uncertain indicator of N_e. Second, the electron number density N_e(S II) so determined cannot probably be used because the S^+ and He^+ regions do not coincide. Therefore we have adopted the following procedure: using the formulae given by Clegg (1987), we have evaluated the electron number density N_e(He II) in such a way that the He I λ5876/λ4471, λ6678/λ4471, and λ7065/λ4471 line ratios have their recombination values, after correction for collisional enhancement. The He I λ7065 line plays an important role because it is particularly density sensitive. This procedure was carried out using Brocklehurst's (1972) and Smits's old (1991a, b) and new (1994) emissivities. Results of the N_e(He II) determinations are shown in Table 5. Brocklehurst's emissivities give higher values of N_e(He II) and therefore larger correction factors $(1 + \gamma)$ because of a smaller λ7065/λ4471 recombination ratio than both sets of Smits' emissivities. Table 5 shows that the self-consistent procedure gives a singly ionized helium abundance y^+ obtained from each of the three He I λ4471, λ5876, and λ6678 lines which does not vary by more than 10 percent in each BCG. Thus we can make use of all three He I lines inthe helium abundance determination, instead of just one or two as is generally the practice in previous work. The weighted mean y^+ of the three independent determinations is also given.

In Figure 3, the λ5876/λ4471 and λ6678/λ4471 singly ionized helium abundance ratios are plotted against temperature before (Figs. 3*a* and 3*c*) and after correction for collisional excitation (Figs. 3*b* and 3*d*). Before correction, there is a very slight positive temperature dependence for the $y^+(5876)/y^+(4471)$ ratio and a very slight negative temperature dependence for the $y^+(6678)/y^+(4471)$ ratio and a clear shift from unity, to ~1.05 for the former and to ~0.95 for the latter. After correction for collisional excitation, the temperature dependence disappears and both ratios scatter about unity. Campbell (1992) did not find a temperature dependence of the uncorrected $y^+(5876)/y^+(4471)$ ratio because, as shown here, this effect is only of the order of 5%, while she was using a heterogeneous data set with a dispersion of ~80%.

Examination of Table 5 shows that the collisional contribution to the helium line intensity increases with electron temperature. Thus for the most metal-deficient BCG, 0940+544N ($Z \sim Z_\odot/35$), this contribution can reach up to 21% in the case of the He I λ5876 line using Brocklehurst's (1972) emissivities, and up to 6% using Smits's old (1991a, b) and new (1994) emissivities.

Some authors prefer to use only the singlet He I λ6678 emission line to determine the primordial helium abundance since this line is less subject to collisional excitation than other He I lines. However this line is weaker than the He I λ4471 line and especially the He I λ5876 line. Moreover, the He I λ6678 line lies near the region of the Earth's atmospheric OH and H_2O absorption bands, rendering its intensity measurement more uncertain. We thus feel it is safest to use all three He I λ4471,

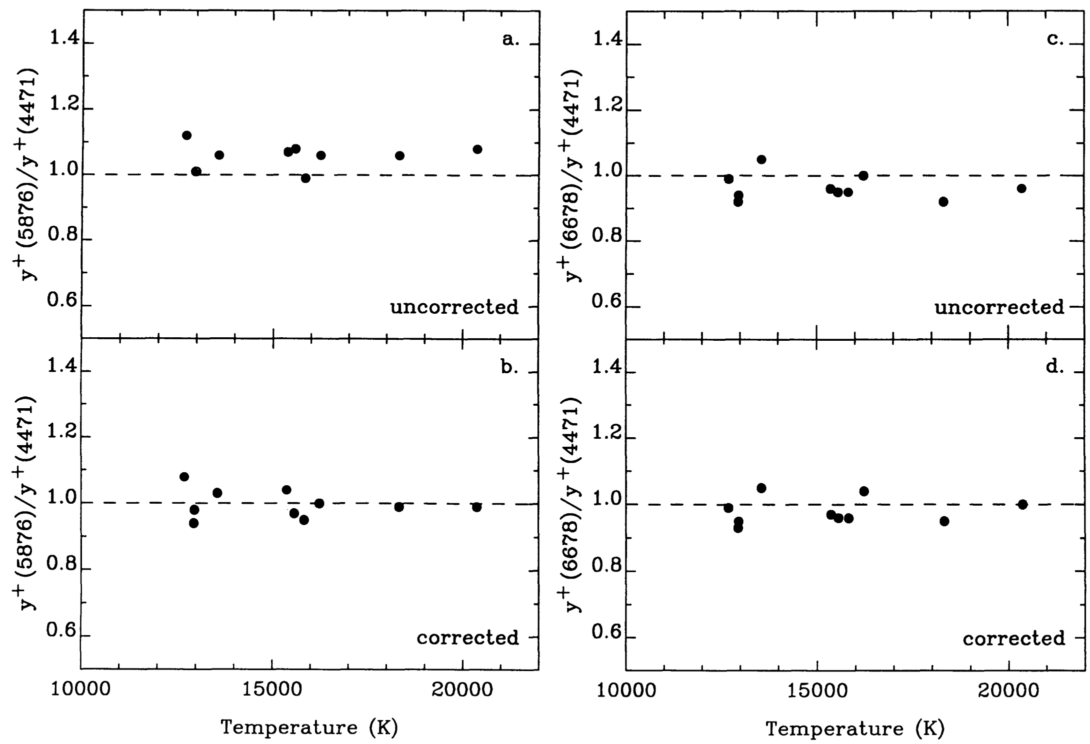

FIG. 3.—Ratio of the (*a*) uncorrected and (*b*) corrected for collisional enhancement (Clegg 1987) singly ionized helium abundance y^+ determined from the He I λ5876 line to that determined from the He I λ4471 line, as a function of electron temperature, for all 10 BCGs. Perfect agreement between the two determinations is shown by the dashed line. Fig. 3*a* shows that the uncorrected y^+(λ5876) is slightly (by about 5%) higher than the uncorrected y^+(λ4471) and that the effect is more important toward higher temperatures. There are only nine points shown, because two points are superposed. After correction for collisional enhancement, the points scatter about the line $y^+(\lambda5876)/y^+(\lambda4471) = 1$, with no trend with electron temperature. Figs. 3*c* and 3*d* show respectively the uncorrected and corrected $y^+(\lambda6678)/y^+(\lambda4471)$ ratios. The uncorrected y^+(λ6678) is slightly smaller (by about 5%) than y^+(λ4471), with the effect becoming more important at higher temperature. Again, correction for collisional enhancement removes both of these effects.

λ5876 and λ6678 lines, corrected for collisional enhancement in a self-consistent manner with the use of the He I λ7065 line.

We note that, in the case of Brocklehurst's (1972) emissivities, the electron number density N_e(He II) based on the requirement that the three He I line intensity ratios λ5876/λ4471, λ6678/λ4471, and λ7065/λ4471 should be pure recombination ratios after correction for collisional enhancement, are far larger than the values obtained from the [S II] λ6717/λ6731 ratio. We have also shown in Table 5 the results for y^+ if we had adopted the electron number densities obtained from the [S II] λ6717/λ6731 ratio. In doing so, we would have underestimated the collisional enhancement and obtained a higher y^+ for all He I lines, but especially for the He I λ5876 line. The effect is most pronounced in the most metal deficient BCGs (such as 0940+544N), where the electron temperature is highest.

Peimbert & Torres-Peimbert (1987a, b) have found that in planetary nebulae, Clegg's (1987) correction factors for He I collisional enhancement can be overestimated by up to a factor of 2. To check the dependence of the singly ionized helium abundance y^+ on Clegg's correction factors γ (eq. [28]), we have calculated y^+ for all three helium lines in the BCG 0940+544N for various values of $\gamma(\lambda)$: $0.5\gamma(\lambda)$, $\gamma(\lambda)$ and $2\gamma(\lambda)$. 0940+544N is the most metal-deficient BCG in our sample and such a dependence should be most visible there. The results of these calculations are shown in Table 6. It is seen that changing $\gamma(\lambda)$ for all lines does modify the electron number density N_e(He II), but not y^+. This insensitivity of y^+ to γ can be understood because our self-consistent procedure relies on He I line ratios, but not on absolute line intensities. Thus, while there may be uncertainties on Clegg's (1987) correction factors and hence on the derived N_e(He II) (doubling γ reduces N_e(He II) by more than a factor of 2), the determination of y^+ is quite robust and does not depend on these uncertainties. The situation is dramatically different if we change γ for only one line. In this case, very different values of y^+ are obtained for one or all He I lines (Table 6). But we consider this case not to be very realistic, since the correction factors for all He I lines are dependent on the helium number density of the common metastable level $2\,^3S$.

Table 6 also shows that, to get better agreement between N_e(He II) and N_e(S II), Clegg's (1987) correction factors have to be increased, *not* decreased as discussed by Peimbert & Torres-Peimbert (1987a, b).

4.3. *Underlying Stellar Absorption*

The next uncertainty in deriving helium abundance comes from the necessity of accounting for the underlying stellar absorption helium lines. Previously this problem has been discussed by Rayo, Peimbert, & Torres-Peimbert (1982), Kunth & Sargent (1983), Peimbert et al. (1986), Dinerstein & Shields (1986), Torres-Peimbert et al. (1989), Pagel et al. (1992), and Skillman & Kennicutt (1993). While Dinerstein & Shields (1986), by assuming a 0.5 Å equivalent width for the underlying He I absorption, derived an upward correction of 10% for the helium abundance in NGC 4861, the other authors found the underlying absorption for the helium lines to be negligible. Since all the helium lines in our BCGs have large equivalent widths (4 to 40 Å), we did not correct the emission helium lines for underlying absorption. To check our procedure, we have plotted in Figure 4 the singly ionized helium abundance y^+, determined separately for each of the He I λ4471 (*asterisks*), λ5876 (*stars*), and λ6678 (*open circles*) lines, as a function of the equivalent width of each line. It is clear from Figure 4 that there is *no* dependence of y^+ on equivalent width, the He I λ4471 line with the lowest equivalent width, and hence, most subject to underlying absorption, having the same mean y^+ as the He I λ5876 line with the largest equivalent width.

We consider next the hypothesis that all helium lines have underlying absorption with an equivalent width of 0.5 Å (Dinerstein & Shields 1986). Since the mean equivalent width of the He I λ4471 emission line is equal to 5 Å, and that of the He I λ6678 line to 10 Å (Fig. 4), by neglecting absorption, we would have underestimated y^+ obtained from the λ4471 line by 10 percent and y^+ obtained from the λ6678 line by 5%. Hence, we would have obtained a mean ratio $y^+(6678)/y^+(4471)$ for all galaxies of about 1.05. But, from Table 5, we derive a mean $y^+(6678)/y^+(4471) = 0.98$. This value has already been corrected for collisional enhancement. Taking into account that the correction for collisional enhancement for the He I λ4471 line is 2%–3% larger than for the He I λ6678 line, the mean observed uncorrected ratio would have been $y^+(6678)/y^+(4471) = 0.96$, 8% lower than the expected ratio corresponding to underlying absorption with an equivalent width of 0.5 Å. We conclude that the true He I absorption equivalent width is much smaller than 0.5 Å.

TABLE 6

DEPENDENCE OF y^+ ON CLEGG'S (1987) CORRECTION FACTORS IN 0940+544N

Correction factor		N_e(HeII) (cm^{-3})	y^+ 4471	5876	6678	mean
γ	for all lines	400	0.077	0.076	0.077	0.076
2γ	for all lines	190	0.077	0.076	0.077	0.076
$\gamma/2$	for all lines	1000	0.077	0.076	0.077	0.076
2γ	for λ7065	140	0.082	0.085	0.080	0.084
$\gamma/2$	for λ7065	350	0.078	0.078	0.077	0.078
2γ	for λ5876	100	0.082	0.082	0.080	0.082
$\gamma/2$	for λ5876	2200	0.063	0.069	0.067	0.067

4.4. *Total Helium Abundance*

To obtain the total helium abundance, the fraction of neutral helium needs to be taken into account. Due to the large difference between the ionization potentials of hydrogen and

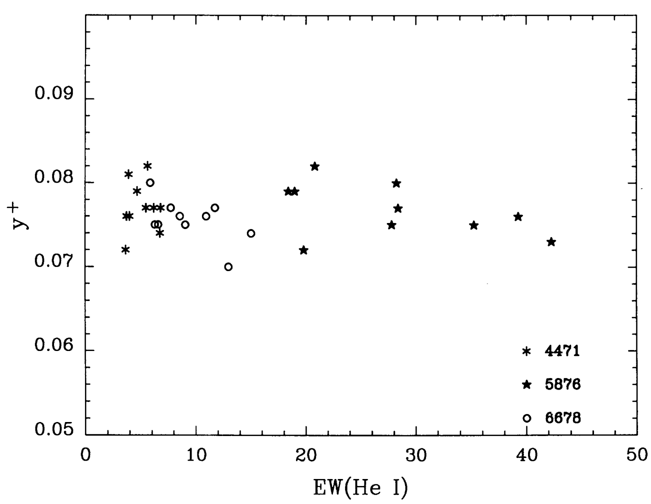

FIG. 4.—Singly ionized helium abundance y^+ corrected for collisional enhancement as a function of the equivalent widths of the He I λ4471 (*asterisks*), λ5876 (*stars*), and λ6678 (*open circles*) emission lines. No trend is seen, suggesting that underlying absorption is negligible.

helium, an H II region can have a significant neutral helium fraction. However, for H II regions with ionizing stars having effective temperatures larger than 40,000 K, the He^+ and H^+ zones are mostly coincident (Stasinska 1990).

The He II λ4686 nebular line was clearly detected in at least three galaxies from our sample. In these cases, the effective temperature of the ionizing stars is larger than 45,000 K. Following Skillman (1989) and Skillman & Kennicutt (1993), we estimate the effective temperatures of the ionizing stars using the oxygen and sulfur ionization fractions. The derived temperatures are all above 55,000 K, except for 1437+370, where we find a value of 50,000 K. Therefore the ionization correction factor for HeI ICF(He) is near unity for all our galaxies.

In Figure 5 we plot the singly ionized helium abundance y^+ as a function of a good indicator of the degree of ionization of the H II region, the fraction of doubly ionized oxygen O^{++}/O. If the correction factor for neutral helium is significant, then there should be a correlation between these two parameters. There is none. Again, we conclude that ICF(He) must be very near unity.

To estimate the small correction factor for neutral helium, we have used the "radiation softness parameter" of Vilchez & Pagel (1988)

$$\eta = \frac{O^+}{S^+}\frac{S^{++}}{O^{++}} . \quad (29)$$

The fraction of neutral helium is significant when $\eta \geq 10$ (Pagel et al. 1992). All our galaxies have $\eta \leq 1$ (Table 5). Nevertheless, using the H II model calculations of Stasinska (1990), we have derived the following dependence of ICF(He) on η

$$\mathrm{ICF(He)} = 1.000 + \eta(0.005 + 0.001\eta) \quad (30)$$

and corrected all helium abundances for He^0. In Figure 6 we have displayed the dependence ICF(He) on η, for low values of η. It is evident that the ICF(He) for all our galaxies does not exceed unity by more than 1.5%.

Additionally, in those cases when the nebular He II λ4686 emission line was detected, we added the abundance of doubly

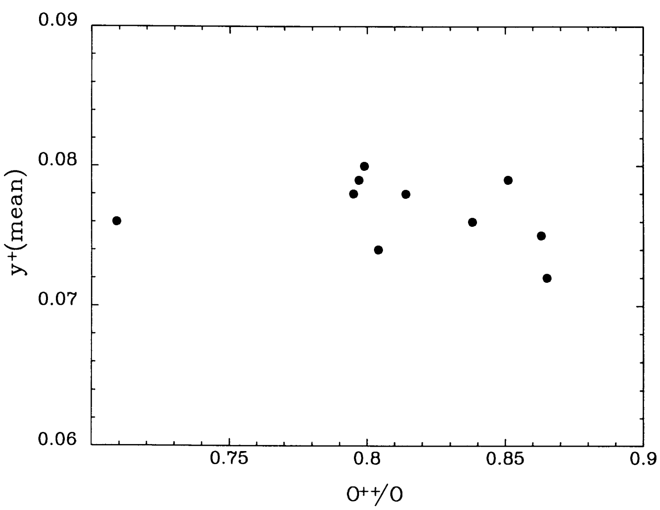

FIG. 5.—Mean singly ionized helium abundance y^+ determined from the He I λ4471, λ5876, and λ6678 lines as a function of the doubly ionized to total oxygen abundance ratio O^{++}/O, an indicator of the galaxy's ionization degree. The absence of correlation between these two quantities implies a negligible fraction of neutral helium to total helium abundance.

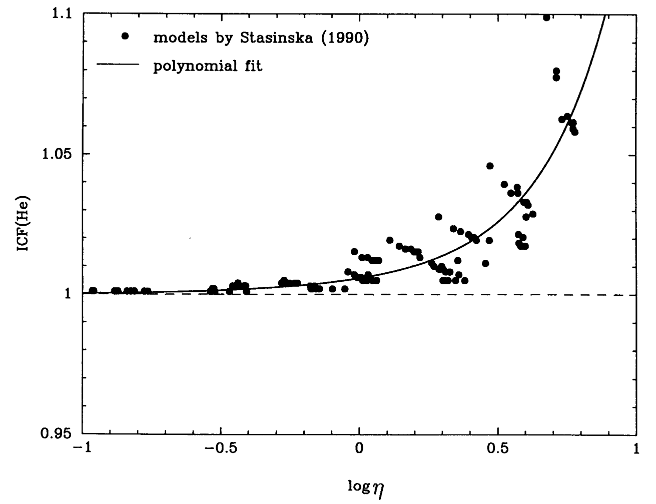

FIG. 6.—Correction factor ICF(He) for neutral helium as a function of the 'softness radiation parameter' $\eta = (O^+/S^+)(S^{++}/O^{++})$ (Vilchez & Pagel 1988) as determined from the grid of photoionization H II region models by Stasinska (1990) (*filled circles*). The solid line represents a polynomial approximation to these models (eq. [30]). All our BCGs have $\log \eta \leq 0.2$ (Table 5) and hence have a correction for neutral He less than ~1.5%.

ionized helium y^{++} to y^+. The value of y^{++} is very small in all cases: it is only 3% of y^+ in 1211+540, and lower than 2% of y^+ in all other galaxies.

Finally the helium mass fraction was calculated by

$$Y = \frac{4y[1 - 20(\mathrm{O/H})]}{1 + 4y} , \quad (31)$$

where y is the number density of helium relative to hydrogen (Pagel et al. 1992). Both y and Y are given in Table 5 for each galaxy.

5. PRIMORDIAL HELIUM ABUNDANCE

There have been two main approaches to determine the primordial helium abundance Y_p: (1) extrapolate empirical linear regressions of the Y versus O/H and Y versus N/H relations to zero metallicity (see e.g., Pagel et al. 1992); (2) take the mean value of the helium abundance in the most metal-deficient BCGs (Kunth & Sargent 1983; Campbell 1992). We employ each of these methods in turn to determine Y_p. In addition to our own data, we shall also be using that of Pagel et al. (1992). In this section, we shall emphasize again that the electron number density in the He^+ region has to be determined in a self-consistent manner to yield the appropriate correction factors for the collisional enhancement of the He recombination lines, and hence the correct Y_p. We shall discuss also the uncertainties introduced in the determination of Y_p by the different sets of emissivity coefficients used.

5.1. *Linear Regressions in the Y versus* O/H *and Y versus* N/H *Planes*

To determine Y_p, Peimbert & Torres-Peimbert (1974, 1976) proposed to extrapolate the following linear relation to zero metallicity:

$$Y = Y_p + \frac{dY}{d(\mathrm{O/H})}(\mathrm{O/H}) . \quad (32)$$

Later Pagel et al. (1986) suggested plotting a regression of

TABLE 7

MAXIMUM-LIKELIHOOD LINEAR REGRESSIONS

Galaxy Sample	Oxygen	Nitrogen
Brocklehurst's (1972) Emissivities		
This paper:		
10 galaxies	0.2288 + 122(O/H)	0.2307 + 3072(N/H)
	±61 ±78	±52 ±2074
6 galaxies without WR	0.2308 + 77(O/H)	0.2327 + 1317(N/H)
	±95 ±181	±68 ±4242
Pagel et al. (1992):		
9 galaxies without WR	0.2291 + 90(O/H)	0.2277 + 3200(N/H)
	±79 ±85	±84 ±2810
19 galaxies without definite WR	0.2279 + 122(O/H)	0.2333 + 1480(N/H)
	±57 ±42	±42 ±550
This paper + Pagel et al. (1992):		
10 + 9 galaxies	0.2296 + 104(O/H)	0.2303 + 2964(N/H)
	±46 ±56	±43 ±1611
10 + 19 galaxies	0.2289 + 116(O/H)	0.2340 + 1438(N/H)
	±35 ±33	±24 ±422
Smits's (1991a, b) Emissivities		
This paper:		
10 galaxies	0.2471 + 77(O/H)	0.2475 + 2352(N/H)
	±63 ±80	±52 ±2045
Smits's (1994) Emissivities		
This paper:		
9 galaxies[a]	0.2394 + 115(O/H)	0.2409 + 3078(N/H)
	±72 ±87	±59 ±2197

[a] The deviant point for 0940 + 544N was excluded from the fit.

helium, not only against oxygen, but also against nitrogen:

$$Y = Y_p + \frac{dY}{d(\mathrm{N/H})}(\mathrm{N/H}) . \qquad (33)$$

These formulae assume a constant mass fraction of oxygen relative to the total heavy element abundance in galaxies with different metallicity. Torres-Peimbert et al. (1989) suggested that it is perhaps preferable to use the total heavy element mass fraction Z, instead of O/H and N/H, to derive linear regressions to take into account variations in C/O and N/O ratios.

We have performed maximum-likelihood linear regressions for our sample of 10 BCGs, using Brocklehurst's (1972) emissivities. The results are given in Table 7. Pagel et al. (1986) have noted that BCGs which show broad spectral features characteristic of Wolf-Rayet (WR) stars often have larger abundances of both helium and nitrogen than objects with the same oxygen abundance, but without WR features. They attributed the enhancement to local pollution by winds of massive stars. To test this hypothesis, we have also performed linear regressions for a subsample of six BCGs where we have excluded the four BCGs in our sample showing obvious broad WR features at He II λ4686. These are 0946 + 558, 0948 + 532, 1135 + 581, and 1437 + 370. 1135 + 581 also shows a broad C IV λ5808 feature, while 1437 + 370 exhibits at least three prominent broad WR features at λ4200, λ4650, and λ5808 (Fig. 2). The latter BCG has a metallicity of $Z_\odot/10$, which places it near the low-metallicity limit of BCGs with detected WR bumps (Masegosa, Moles, & del Olmo 1991). The fit parameters for the subsample without WR galaxies are not significantly different from those for the entire sample, so we conclude that we do not have to exclude WR galaxies in the determination of the primordial helium abundance. Our WR galaxies do not appear to show the pollution effect discussed by Pagel et al. (1986). If anything, removing the WR galaxies yields a slightly higher Y_p, opposite to the sense expected for pollution effects. For comparison, we have also shown the results for the sample of nine galaxies without WR features and for that which includes an additional 10 galaxies without known information about WR features from Pagel et al. (1992). As Table 7 shows, there is no significant difference between the regression relations for our and the Pagel et al. (1992) data. Therefore we have combined to the two data sets to improve the statistics. The results of the fits for the combined data are also shown. The data for our sample (*filled circles*) along with the nine galaxies without WR features of Pagel et al. (1992) (*open circles*) are shown in Figure 7 in both the Y versus O/H (Fig. 7*a*) and Y versus N/H (Fig. 7*b*) planes. The solid line is the maximum-likelihood linear regression lines, while the dashed lines show alternatives equivalent to $\pm 1\,\sigma$ limits.

To illustrate the effects of the uncertainties in the atomic data on the determination of the primordial helium abundance, we show in Figure 8 our data, calculated with Smits's old (1991a, b) emissivities, and the corresponding linear regression fits in both the Y versus O/H (Fig. 8*a*) and Y versus N/H (Fig. 8*b*) planes. The Pagel et al. (1992) data could not be used because they were derived with only Brocklehurst's (1972) emissivities. Figure 9 displays the same data and fits, but calculated with Smits's new (1994) emissivities. In deriving the fits in Figure 9, we have excluded the point for the galaxy 0940 + 544N which lies further apart from the other points.

Comparison of the results for our and the Pagel et al. samples (Table 7) shows that the results for Y_p, dY/d(O/H) and dY/d(N/H) for these independent samples (there are no common galaxies) are in excellent agreement. While this agreement may appear at first very rewarding, it is in fact rather

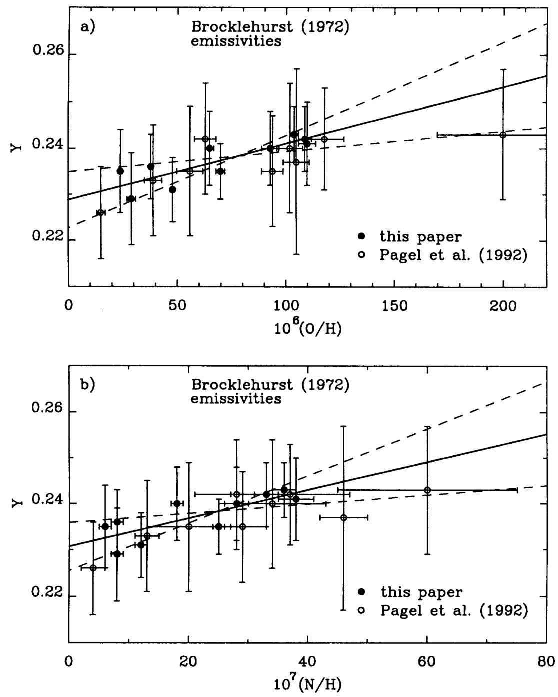

FIG. 7.—Linear regressions of the helium mass fraction Y calculated with Brocklehurst's (1972) emissivities and electron number densities determined self-consistently from the He I $\lambda5876/\lambda4471$, $\lambda6678/\lambda4471$, and $\lambda7065/\lambda4471$ lines ratios, vs. (*a*) oxygen and (*b*) nitrogen abundances for the galaxies from this paper (*filled circles*). Maximum-likelihood regression lines (*solid line*) are shown along with alternatives (*dashed lines*) equivalent to $\pm1\ \sigma$ limits. The nine galaxies without detected Wolf-Rayet features from Pagel et al. (1992) (*open circles*) are also shown for comparison.

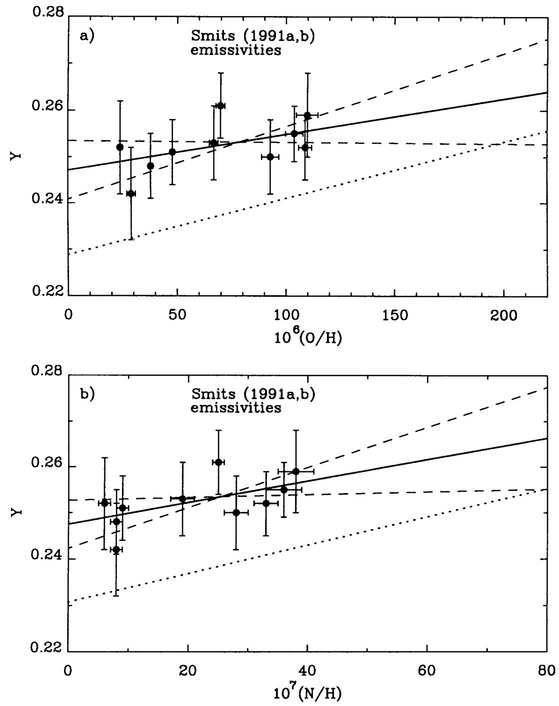

FIG. 8.—Linear regression of the helium mass fraction Y calculated with Smits' (1991a, b) old emissivities and electron number densities determined self-consistently from the He I $\lambda5876/\lambda4471$, $\lambda6678/\lambda4471$,)nd $\lambda7065/\lambda4471$ line ratios, vs. (*a*) oxygen and (*b*) nitrogen abundances. Linear regression lines (*solid lines*) are shown along with alternatives (*long-dashed lines*) equivalent to $\pm1\ \sigma$ limits. For comparison, the fit in Figure 7, obtained using Brocklehurst's (1972) emissivities is also shown (*short-dashed lines*). All points are systematically shifted higher, and the derived primordial helium abundance using Smits's emissivities is $\sim7\%$ higher than when using Brocklehursts's emissivities. Note also that the dispersion of the data points in the Y vs. O/H and Y vs. N/H planes is higher than in Fig. 7.

puzzling because, although we have used the same formulae for abundance determinations as Pagel et al. (1992), we differ from these authors in three important respects:

(1) To correct for collisional enhancement of the He I lines, we used N_e(He II) derived in a self-consistent manner by requiring that the He I $\lambda5876/\lambda4471$, $\lambda6678/\lambda4471$, and $\lambda7065/\lambda4471$ line ratios to have their recombination values after correction for collisional enhancement. Instead, Pagel et al. (1992) use N_e(S II) determined from the [S II] $\lambda6717/\lambda6731$ ratio.

(2) For all galaxies in our sample, all three He I $\lambda4471$, $\lambda5876$, and $\lambda6678$ lines were used to determine y^+. Individual values of these lines never differ from the mean by more than $\sim7\%$. This is in contrast to Pagel et al. (1992) who use in the majority of cases only two or one lines (usually the less collisionally sensitive He I $\lambda4471$ and $\lambda6678$ lines) for the determination of y^+.

(3) Pagel et al. (1992) do not correct for neutral helium. But as we have seen, this correction factor is small, less than $\sim1\%$.

There is a fourth difference. We use, for the S^{++} abundance determination, the electron temperature defined by Garnett (1992) instead of T_e(O III) used by Pagel et al. (1992). However, this difference does not affect significantly the helium abundance determination.

We now discuss the effects of the first two main procedural differences on the helium abundance determination. Using the [S II] $\lambda6717/\lambda6731$ ratio yields in most cases only upper limits for the electron density, and thus introduces an uncertainty in the correction factor for the He I collisional enhancement. This uncertainty is unimportant for metal-rich low-temperature ($T_e \sim 10{,}000$ K) galaxies which have a small weight in the primordial He abundance Y_p determination, and where the correction factors are small. But it may substantially affect the results for helium abundance determination in low-metallicity high-temperature ($T_e \sim 20{,}000$ K) BCGs (like the ones discussed here) which have a large weight in the Y_p determination and where the correction factors are large.

To illustrate the uncertainty introduced by using a wrong collisional enhancement correction factor, we have also given in Table 5 y^+ calculated with N_e(He II) set equal N_e(S II) for all our BCGs. It is clear that the y^+ have systematically higher values, by as much as 10%. Using the correction factors for He I collisional enhancement calculated with N_e(S II) *overestimates* Y_p.

Thus how do we explain the excellent agreement between our and the Pagel et al. (1992) Y-values (Fig. 7)? We cannot reproduce the exact procedure used by Pagel et al. (1992) in their helium abundance determination because there are not enough details given in their paper. But we suspect that for most galaxies, Pagel et al. (1992) gave the most weight to the least density dependent line, the He I $\lambda6678$ line. For this line, the collisional enhancement factor is small, and the exact value of the electron density used to calculate it does not matter as much. To check this hypothesis, we have plotted in Figure 10*c* against O/H the Y-values obtained for our BCGs from the He I $\lambda6678$ line, using N_e(He II) = N_e(S II) and without correcting for neutral helium, to follow the procedure used by Pagel et al. (1992). We see that there is indeed excellent agreement between

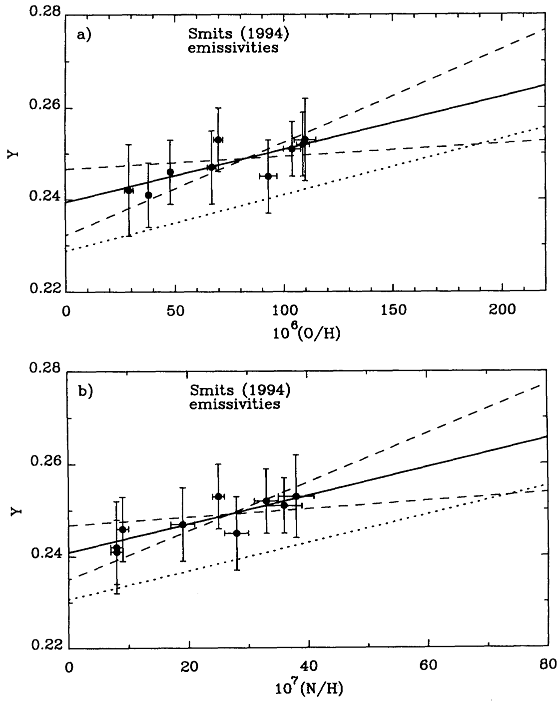

FIG. 9.—Same as Fig. 8, except that Smits's (1994) new emissivities are used. The derived primordial helium abundance is ~4% higher than when using Brocklehurst (1972)'s emissivities. The dispersion of the data points in the Y vs. O/H and Y vs. N/H planes is similar to that in Fig. 7.

the Pagel et al. data (*open circles*) and our data (*filled circles*). The best fit line from Figure 7*a* is also shown and it does fit well all data points. In Figures 10*a* and 10*b*, we show the same diagram, but with Y determined from each of the He I λ4471 and λ5876 lines, respectively. These lines are more density dependent, and all our data points are now shifted upward relative to the Pagel et al. data and the best-fit line in Figure 7*a*. For the Y-values determined from the most density-dependent He I λ5876 line, the shift can be as much as 5%. Finally we show in Figure 10*d*, the Y-values determined from the weighted average of all three He I λ4471, λ5876, and λ6678 lines. As expected, all our points are also shifted upward relative to the best-fit line in Figure 7*a* and the Pagel et al. data. The same trends are seen when the Y-values are plotted against N/H.

We thus conclude that, to obtain an accurate helium abundance determination with the use of as many He lines as possible, it is crucially important to determine precisely the correction factor for collisional enhancement of the He I lines. We feel that our self-consistent procedure described above permits to do just that.

Examination of the parameters of the regression fits in Table 7 shows that, for a given set of emissivities, Brocklehurst's in this case, the determination of Y_p is quite robust. It depends neither on the particular galaxy sample considered, nor on whether the regression of helium against oxygen or nitrogen is used. Taking the mean of the intercepts of both regression lines at O/H = N/H = 0, our sample gives $Y_p = 0.229 \pm 0.004$. This is in excellent agreement with the value obtained by Pagel et al.

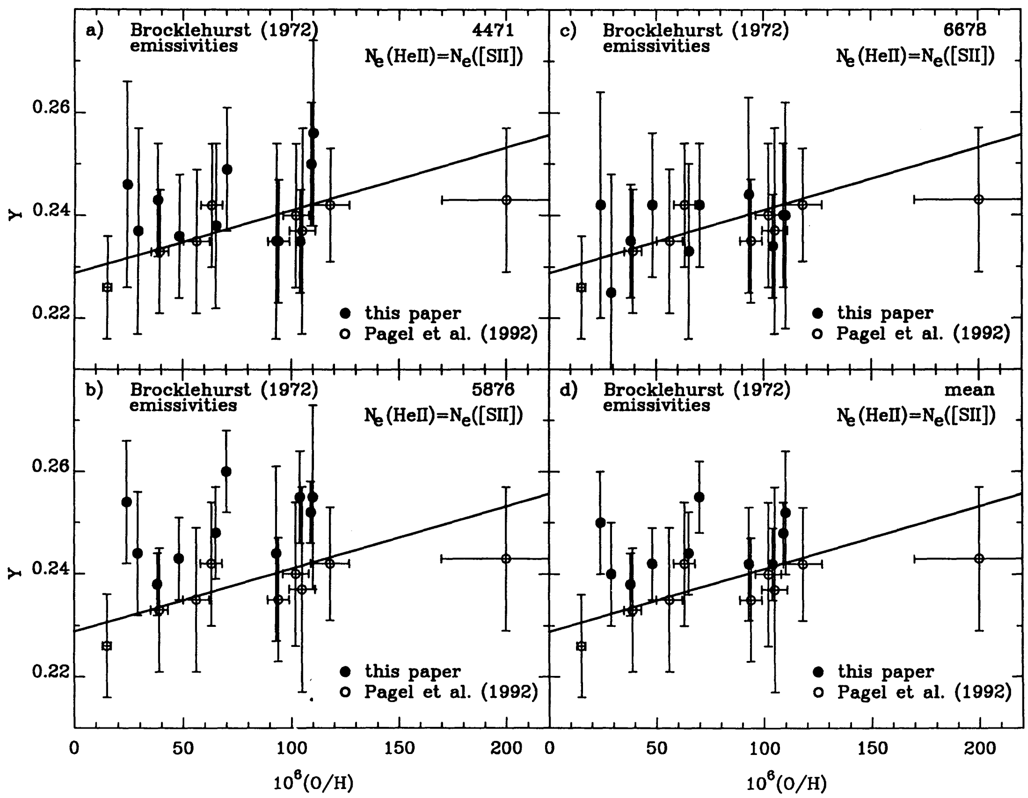

FIG. 10.—Helium mass fraction Y calculated for our data (*filled circles*) with the electron number density obtained from the [S II] λ6717/λ6731 ratio, vs. oxygen abundance. Y has been derived using, respectively, (*a*) the He I λ4471 line, (*b*) the He I λ5876 line, (*c*) the He I λ6678 line, and (*d*) the weighted mean of all three preceding lines. The agreement between our and Pagel et al. (1992) data [also obtained using N_e(He II) = N_e(S II)] (*open circles*) and the best-fit line in Fig. 7 (*solid line*) is best in the case of the He I λ6678 line (Fig. 9*c*) which is least sensitive to collisional enhancement and gets progressively worse (our data are shifted higher) when the other lines He I λ4471 (Fig. 9*a*) and λ5876 (Fig. 9*b*) are used. Fig. 9*d* shows that using N_e(He II) = N_e(S II) and the weighted mean of all three lines can overestimate the primordial helium abundance by as much as 5%.

(1992) with a totally different galaxy sample $Y_p = 0.228 \pm 0.005$. Combining our data with that of Pagel et al. (1992), slightly reduces the errors bars: $Y_p = 0.229 \pm 0.003$. The robustness of the determination of Y_p results from the fact that we have added a significant number of very low-metallicity objects to the Y versus O/H and Y versus N/H diagrams and that our spectral data are of high quality giving small error bars. The high quality of the data also allows to say that there is *not* an increase in the dispersion of Y for low O/H and N/H (Fig. 7). Had we calculated the collisional enhancement factor with N_e(S II), our sample would have given $Y_p = 0.241 \pm 0.012$ for the Y versus O/H regression line (Fig. 9*d*) and $Y_p = 0.241 \pm 0.010$ for the Y versus N/H regression line. We would have overestimated Y_p by $\sim 5\%$.

We discuss next how the use of a particular set of He I recombination emissivities effect the determination of Y_p. There is a significant discrepancy between the old He I emissivity calculations of Smits (1991a, b) and those of Brocklehurst (1972) for the He I $\lambda 4471$, $\lambda 5876$, and $\lambda 6678$ lines at electron temperatures relevant for metal-deficient BCGs ($T_e \sim 20{,}000$ K). The new Smits emissivities (1994) agree well with those of Brocklehurst for these three lines, but are higher by $\sim 35\%$ for the He I $\lambda 7065$ line. Skillman & Kennicutt (1993) found that, using only the He I $\lambda 6678$ line, the helium abundance of the BCG I Zw 18 is increased by $\sim 4\%$ with Smits's old (1991a, b) emissivities, as compared with Brocklehurst's emissivities. Using all three He I $\lambda 4471$, $\lambda 5876$, and $\lambda 6678$ lines, we found that the Y-values of our BCGs can be pushed upward by as much as 10% when Smits' old (1991a, b) emissivities are used instead of Brocklehurst's (Fig. 8 and Table 5) and by as much as 8% when Smits's new (1994) emissivities are used. This increase in Y is caused by two factors: (1) smaller Smits old (1991a, b) emissivities and (2) a larger He I $\lambda 7065/\lambda 4471$ recombination ratio for both old (1991a, b) and new (1994) Smits emissivities, which leads to a smaller N_e(He II) and hence to a smaller correction factor for collisional enhancement. Table 7 shows that the Y_p derived using the old Smits emissivities and taking the mean of the O/H and N/H determinations is 0.247 ± 0.004, higher by $\sim 7\%$ than the Y_p derived with Brocklehurst's emissivities. If we use the new set of Smits emissivities, we obtain $Y_p = 0.240 \pm 0.005$, higher by $\sim 4\%$ than Y_p determined with Brocklehurst's emissivities.

Comparison of Figures 7, 8, and 9 and examination of Table 5 show that the data exhibit a larger dispersion in the Y versus O/H and Y versus N/H planes, and that the spread in Y values from individual He lines in the same object is more pronounced with the old Smits (1991a, b) emissivities than with Brocklehurst's. We thus conclude that Brocklehurst's values are more accurate than Smits's (1991a, b) old emissivities. If we use Smits's new emissivities, the dispersion of the data points in the Y verus O/H (Fig. 9*a*) and Y versus N/H (Fig. 9*b*) planes (excluding the point for 0940+544N which is deviant) and of Y-values from individual He lines in the same object (Table 5) is similar to that obtained with Brocklehurst's emissivities.

As for the slopes of the regression lines, we obtain, using Brocklehurst's (1972) emissivities, $dY/d(\mathrm{O/H}) = 122 \pm 78$ and $dY/d(\mathrm{N/H}) = 3072 \pm 2074$ for our sample, $dY/d(\mathrm{O/H}) = 116 \pm 33$ and $dY/d(\mathrm{N/H}) = 1438 \pm 422$ for our sample combined with the 19 galaxies of Pagel et al. If we assume $Z = 20(\mathrm{O/H})$, then the latter value of $dY/d(\mathrm{O/H})$ corresponds to $dY/dZ = 5.8 \pm 1.7$ consistent with the values of 6.1 ± 2.1 of Pagel et al. (1992) and 3 of Lequeux et al. (1979) and Peimbert (1985). With Smits's old emissivities, $dY/dZ = 3.9 \pm 4.0$ while Smits's new emissivities give $dY/dZ = 5.8 \pm 4.4$. All these dY/dZ are higher than the theoretical values of 0.5–2.0 predicted by closed box chemical evolution models with a Salpeter slope for the initial mass function (Campbell 1992; Marconi et al. 1994).

5.2. *Mean of Lowest Metallicity BCGs*

The linear extrapolations of the Y versus O/H and Y versus N/H regression lines to O/H = N/H = 0 to determine Y_p, as discussed above, have only an empirical basis. When the data are of high quality (as is the case here), the dispersion about a linear fit to those two relations is observationally small (see Fig. 7) and it is empirically justified to use a linear extrapolation for the determination of Y_p. But there is, as yet, no theoretical basis for such a linear relationship. It is thought that helium is produced by stars of any initial mass, oxygen by massive stars ($M \geq 8\ M_\odot$), primary nitrogen by a restricted range of intermediate mass stars experiencing envelope burning ($3\ M_\odot \leq M \leq 8\ M_\odot$) and secondary nitrogen mostly by intermediate-mass stars and a little by massive stars. Because of the different nucleosynthesis timescales in these stars with different masses, Y is not expected to be proportional to either O/H or N/H.

Moreover, BCGs are expected not to be closed-box systems, but to lose mass by galactic winds set up by supernovae. In fact, chemical evolution models with differential galactic winds (Pilyugin 1993; Marconi et al. 1994) where oxygen is lost far more efficiently than helium and nitrogen, predict values of dY/dZ in the range 2–15, in far better agreement with the observations than those given by closed-box models. In these models with differential galactic winds, the track of a BCG in the Y versus O/H and Y versus N/H planes is not a straight or even a smooth line. Due to the self-enrichment of the H II regions associated with the star-forming bursts, and the random variations of the efficiencies of the heavy element enriched galactic winds from one starburst to another, depending on the location of the burst and the geometry of the galaxy, the evolutionary track describes an irregular sawtooth curve.

Thus some authors (e.g., Kunth & Sargent 1983) have abandoned the linear extrapolation method and have preferred to determine Y_p by taking the mean of the helium abundances in the most metal-deficient known galaxies. This can be justified by the fact that, in a BCG undergoing a burst of star formation, the gas is quickly enriched with oxygen, while the helium abundance changes much more slowly, making the galaxy move horizontally across the Y versus O/H plane.

The number of known BCGs with very low metallicity, say less than $Z_\odot/15$, is very small. We have added four more such objects in this work, doubling their number: 0940+544N ($Z_\odot/35$, $Y = 0.235 \pm 0.009$), 1159+545 ($Z_\odot/29$, $Y = 0.229 \pm 0.010$), 0832+699 ($Z_\odot/21$, $Y = 0.236 \pm 0.007$), and 1211+540 ($Z_\odot/17$, $Y = 0.231 \pm 0.007$). Taken the error weighted mean gives $Y_p = 0.233 \pm 0.003$, where the error denotes the standard deviation from the mean. If we now add the four other known BCGs with $Z < Z_\odot/15$: I Zw 18 ($Z_\odot/50$, $Y = 0.231 \pm 0.006$, Skillman & Kennicutt 1993), SBS 0335−052B ($Z_\odot/41$, $Y = 0.233 \pm 0.016$, Melnick et al. 1992), Tol 65 ($Z_\odot/21$, $Y = 0.231 \pm 0.016$, Pagel et al. 1992) and T1214−277 ($Z_\odot/21$, $Y = 0.233 \pm 0.012$, Pagel et al. 1992), then the weighted mean gives: $Y_p = 0.232 \pm 0.002$. From this data set, there is no BCG known with a Y significantly below 0.232. The value obtained for Y_p is slightly larger than that obtained from the linear regression method ($Y_p = 0.229 \pm 0.004$), but is still consistent with it within the errors. All the above Y-values have been obtained using Brocklehurst's (1972) emissivities. If we use Smits's new emissivities, taking the error weighted mean of the Y of the four most metal-deficient BCGs in our sample gives $Y_p = 0.245 \pm 0.004$.

The Y_p-value calculated with Brocklehurst's emissivities and obtained by linear regression is 1.8 σ lower than the lower limit $Y_p = 0.236$ predicted by SBBN, while that obtained by the mean of the most metal-deficient BCGs is 2 σ lower. The Y_p-values obtained with both methods using Smits's new (1994) emissivities are fully consistent with that lower limit. If we make allowance for systematic errors which may amount to 0.005, the primordial helium mass fraction determined here, with either Brocklehurst's or Smits's emissivities, is consistent with SBBN, and leads to the well-known cosmological limits: a neutron half-life less than 10.4 minutes, a number of neutrino species less than 3.2, and a baryonic mass density $\Omega_{b0} h_{100}^2 < 0.016$, where Ω_{b0} is the fraction of the closure density in baryons and h_{100} is the Hubble constant in units of 100 km s^{-1} Mpc^{-1} (Pagel et al. 1992). The first two limits have been confirmed experimentally. The neutron half-life has been measured to be $\tau_n = 10.25$ mn (e.g., Mampe et al. 1989) and the number of neutrino species to be $N_\nu = 3.01 \pm 0.10$ (Pagel et al. 1992).

We finally note that for the eight lowest metallicity BCGs known, 12 + log (O/H) ranges between 7.2 and 7.6 and log (N/O) ranges from -1.5 to -1.7. Using Pilyugin's (1993) models, these ranges of O/H and N/O give an efficiency of the enriched galactic wind, defined as the ratio of the mass of supernovae ejecta leaving the galaxy to the total mass of supernovae ejecta, of $\geq 50\%$.

6. CONCLUSIONS

We present in this paper spectrophotometric observations with high signal-to-noise ratio of 10 low-metallicity blue compact galaxies selected mainly from the First and the Second Byurakan surveys. We use these high-quality data to determine the primordial helium abundance.

We have obtained the following main results:

1. The oxygen abundance in our BCGs ranges from 12 + log (O/H) = 7.37 to 8.04, a range large enough to allow a precise determination of the primordial helium abundance from a homogeneous data set. There are four galaxies in our sample with $Z < Z_\odot/15$, thus doubling the known number of very metal-deficient BCGs. The most metal-deficient BCGs in our sample, 0940+544N and 1159+545, have, respectively, $Z_\odot/35$ and $Z_\odot/29$.

2. We found the underlying absorption for the He lines to be negligible. Self-absorption effects on the He I λ4471, λ5876 and λ6678 lines used for helium abundance determination, are also found to be insignificant.

3. The correction factor for neutral helium does not exceed 1% for all BCGs. It is inferior to 3% for He^{++} in all galaxies.

4. The main physical mechanism changing the He I line intensities from their recombination values is collisional excitation of the He I lines from the metastable levels $2\,^3S$ and $2\,^1S$. To correct for it, we set T_e(He II) = T_e(O III) and derive the electron number density in the He^+ zone by a self-consistent procedure which constrains the He I λ5876/λ4471, λ6678/λ4471, and λ7065/λ4471 line ratios to have their recombination values, after correction for collisional enhancement. This method gives a robust determination of the helium abundance which is insensitive to both uncertainties in the collisional correction factors and the derived electron number density. The usual practice of using N_e as derived from the [S II] λ6717/λ6731 ratio systematically underestimates the collisional enhancement correction factors for the He I lines and hence overestimates the derived helium abundance.

5. Extrapolation to O/H = N/H = 0 of the linear regressions Y versus O/H and Y versus N/H for our BCG sample and using Brocklehurst's (1972) emissivities gives a primordial helium mass fraction $Y_p = 0.229 \pm 0.004$. Taking the mean Y of the four most metal-deficient ($Z < Z_\odot/15$) BCGs in our sample gives $Y_p = 0.233 \pm 0.003$. Adding the four most metal-deficient BCGs known from the literature ($Z < Z_\odot/15$) yields $Y_p = 0.0232 \pm 0.002$. There is no BCG known with a Y significantly below 0.232.

Using Smits's old (1991a, b) and new (1994) emissivities instead of Brocklehurst's (1972) leads to a higher primordial helium abundance by about 7% ($Y_p = 0.247 \pm 0.004$) and 4% ($Y_p = 0.240 \pm 0.005$), respectively. Brocklehurst's values are better than Smits's old emissivities in the sense that they lead to less dispersion of the data points in the Y versus O/H and Y versus N/H planes and in the helium abundances derived from different He I lines in a given galaxy. On the other hand, Smits's new emissivities give a comparable dispersion to that obtained with the Brocklehurst values. The determined Y_p with either Brocklehurst's (1972) or Smits's (1991a, b, 1994) emissivities are consistent with the lower limit $Y_p = 0.236$ required by standard big bang nucleosynthesis theory.

6. Our BCG sample gives a slope of the Y versus O/H linear regression $dY/dZ = 6.1 \pm 3.9$ using Brocklehurst's (1972) emissivities. Adding the data of Pagel et al. (1992) yields $dY/dZ = 5.8 \pm 1.7$. Using Smits's (1991a, b) old emissivities gives $dY/dZ = 3.9 \pm 4.0$, while using Smits's (1994) new emissivities gives $dY/dZ = 5.8 \pm 4.4$. These slopes are larger than the values of 0.5–2.0 predicted by closed-box models, but are consistent with those given by chemical evolution models with differential galactic winds, and a wind efficiency defined as the ratio of the mass of supernovae ejecta leaving the galaxy to the total mass of supernovae ejecta, greater than $\sim 50\%$ for the most metal-deficient BCGs.

Y.I.I. has been supported in part by the Ukrainian State Committee for Science and Technology and by grant No. A-02-037 of the ESO Central and Eastern Europe Program. T.X.T. acknowledges the partial financial support from Air Force Office for Scientific Research grant AFOSR 89-0467, from a fellowship of the Ministere de la Recherche et de la Technologie and from a Visiting Professorship at the University of Paris VII. This international collaboration has been made possible by the award of the 1992 Henri Chrétien Award by the American Astronomical Society and of NATO collaborative research grant no. 921285. V.A.L. was supported in part by a grant from the US National Academy of Sciences in the Program for Collaboration in Basic Science and Engineering. He thanks R. Green and the staff of NOAO for their kind hospitality. Special thanks are due to J. de Veny for assistance with the operation of the RC spectrograph, and to J. Barnes for help with the processing with IRAF. Y.I.I. and T.X.T. thank Chantal Balkowski for her warm hospitality at the Departement d'Astronomie extragalactique et de Cosmologie at the Observatoire de Paris-Meudon. The authors are grateful to A. Kniazev and A. Ugryumov for their assistance with the processing of the spectra with the MIDAS software package. We thank D. Kunth, J.-P. Meyer, and L. Pilyugin for discussions and S. Torres-Peimbert for prompting us to recalculate our helium abundances with the new set of emissivities which D. Smits kindly provided in advance of publication.

REFERENCES

Aller, L. H. 1984, Physics of Thermal Gaseous Nebulae (Dordrecht: Reidel)
Brocklehurst, M. 1971, MNRAS, 153, 471
———. 1972, MNRAS, 157, 211
Campbell, A. 1992, ApJ, 401, 157
Campbell, A., Terlevich, R., & Melnick, J. 1986, MNRAS, 223, 811
Clegg, R. E. S. 1987, MNRAS, 229, 31P
Davidson, K., & Kinman, T. D. 1985, ApJS, 58, 321
Dinerstein, H., & Shields, G. 1966, ApJ, 311, 45
Dufour, R. J., Garnett, D. R., & Shields, G. A. 1988, ApJ, 332, 752
French, H. B. 1980, ApJ, 240, 41
Garnett, D. 1990, ApJ, 363, 142
———. 1992, AJ, 103, 1330
Garstang, R. H., Robb, W. D., & Rountree, S. P. 1978, ApJ, 222, 384
Hummer, D. G., & Storey, P. J. 1987, MNRAS, 224, 801
Izotov, Yu. I., Lipovetsky, V. A., Guseva, N. G., & Stepanian, J. A. 1990a, AZhPis'ma, 16, 605
Izotov, Yu. I., Lipovetsky, V. A., Guseva, N. G., Kniazev, A. Yu., & Stepanian, J. A. 1990b, Nature, 343, 238
———. 1991, A&A, 247, 303
Izotov, Yu. I., Lipovetsky, V. A., Guseva, N. G., Kniazev, A. Yu., Neizvestny, S. I., & Stepanian, J. A. 1992a, Astron. Astrophys. Trans., 3, 193
Izotov, Yu. I., Lipovetsky, V. A., Guseva, N. G., & Kniazev, A. Yu. 1992b, in The Feedback of Chemical Evolution on the Stellar Content of Galaxies, ed. D. Alloin & G. Stasinska (Paris: Paris Obs. Publ.), 138
Izotov, Yu. I., Guseva, N. G., Karachentsev, I. D., & Karachentseva, V. E. 1992c, Astron. Astrophys. Trans., 1, 283
Kinman, T. D., & Davidson, K. 1981, ApJ, 243, 147
Kunth, D., & Sargent, W. L. W. 1983, ApJ, 273, 81
Lequeux, J., Peimbert, M., Rayo, J. F., Serrano, A., & Torres-Peimbert, S. 1979, A&A, 80, 155
Mampe, W., Ageron, P., Bates, C., Pendlebury, J. M., & Steyerl, A. 1989, Phys. Rev. Lett., 63, 593
Marconi, G., Matteucci, F., & Tosi, M. 1994, MNRAS, in press
Markarian, B. E. 1967, Astrofizika, 3, 55
———. 1969, Astrofizika, 5, 443
Markarian, B. E., & Lipovetsky, V. A. 1972, Astrofizika, 8, 155
Markarian, B. E., Lipovetsky, V. A., & Stepanian, J. A. 1981, Astrofizika, 17, 619
———. 1983, Astrofizika, 19, 29
Markarian, B. E., Lipovetsky, V. A., Stepanian, J. A., Erastova, L. K., & Shapovalova, A. I. 1989, Comm. Special Astrophys. Obs. USSR, 62, 5
Masegosa, J., Moles, M., & del Olmo, A. 1991, AA, 249, 505
McCall, M. L. 1984, MNRAS, 208, 253
McCall, M. L., Rybski, P. M., & Shields, G. A. 1985, ApJS, 57, 1
Melnick, J., Heydary-Malayeri, M., & Leisy, P. 1992, A&A, 253, 16
Olive, K. A., Schramm, D. N., Steigman, G., & Walker, T. P. 1990, Phys. Lett. B, 236, 454
Pagel, B. E. J., & Simonson, E. A. 1991, Rev. Mexicana Astron. Af., 18, 153
Pagel, B. E. J., Simonson, E. A., Terlevich, R. J., & Edmunds, M. G. 1992, MNRAS, 255, 325
Pagel, B. E. J., Terlevich, R. J., & Melnick, J. 1986, PASP, 98, 1005
Peimbert, M. 1985, in Star-Forming Dwarf Galaxies and Related Objects, ed. D. Kunth, T. X. Thuan, & J. T. T. Van (Gif-sur-Yvette: Éditions Frontières), 403
Peimbert, M., Peña, M., & Torres-Peimbert, S. 1986, A&A, 158, 266
Peimbert, M., & Torres-Peimbert, S. 1974., ApJ, 193, 327
———. 1976, ApJ, 203, 581
———. 1987a, Rev. Mexicana Astron. Af. 14, 540
———. 1987b, Rev. Mexicana Astron. Af., 15, 117
Pilyugin, L. S. 1993, A&A, 277, 42
Rayo, J. F., Peimbert, M., & Torres-Peimbert, S. 1982, ApJ, 255, 1
Robbins, R. R. 1968, ApJ, 151, 511
Roy, J.-R., Aube, M., McCall, M. L., & Dufour, R. J. 1992, ApJ, 386, 498
Salzer, J. J., MacAlpine, G. M., & Boroson, T. A. 1989, ApJS, 70, 479
Searle, L., & Sargent, W. L. W. 1972, ApJ, 173, 25
Skillman, E. 1989, ApJ, 347, 883
Skillman, E., & Kennicutt, R. C., Jr. 1993, ApJ, 411, 655
Smits, D. P. 1991a, MNRAS, 248, 193
———. 1991b, MNRAS, 251, 316
———. 1994, private communication
Stasinska, G. 1990, A&AS, 83, 501
Terlevich, R. J., & Melnick, J. 1981, MNRAS, 195, 839
Terlevich, E., Terlevich, R., Skillman, E., Stepanian, J., & Lipovetsky, V. 1991, in Elements and the Cosmos, ed. M. G. Edmunds & R. J. Terlevich (Cambridge: Cambridge Univ. Press), 21
Thuan, T. X. 1991, in Massive Stars in Starbursts, ed. C. Leitherer, N. R. Walborn, T. M. Heckman & C. A. Norman (Cambridge: Cambridge Univ. Press), 183
Thuan, T. X., Izotov, Yu. I., Lipovetsky, V. A. & Pustil'nik, S. A. 1994, in Proc. ESO/OHP Workshop on Dwarf Galaxies (Garching: ESO), in press
Torres-Peimbert, S., Peimbert, M., & Fierro, J. 1989, ApJ, 345, 186
Vilchez, J. M., & Pagel, B. E. J. 1988, MNRAS, 231, 257
Vilchez, J. M., Pagel, B. E. J., Diaz, A., Terlevich, E., & Edmunds, E. 1988, MNRAS, 235, 633
Walker, T. P., Steigman, G., Schramm, D. N., & Olive, K. A. 1991, ApJ, 376, 51
Whitford, A. E. 1958, AJ, 63, 201